Since January 2020 Elsevier has created a COVID-19 resource centre with free information in English and Mandarin on the novel coronavirus COVID-19. The COVID-19 resource centre is hosted on Elsevier Connect, the company's public news and information website.

CHAPTER ONE

Improving properties of the nucleobase analogs T-705/T-1105 as potential antiviral

Xiao Jia, Benedikt Ganter, and Chris Meier*
Organic Chemistry, Department of Chemistry, Faculty of Mathematics, Informatics and Natural Sciences, Universität Hamburg, Hamburg, Germany
*Corresponding author: e-mail address: chris.meier@chemie.uni-hamburg.de

Contents

1. Introduction

In recent years, RNA viruses have become a significant threat to public health because of apparent sudden epidemic outbreaks and periodic pandemics, which cause considerable medical and socioeconomic burden.[1] These viruses, many of them causing so-called emerging infections, such as Ebola, Influenza, and Zika, are highly transmissible and cause immense

Annual Reports in Medicinal Chemistry, Volume 57
ISSN 0065-7743
https://doi.org/10.1016/bs.armc.2021.08.002

morbidity and mortality.[2–4] The newly emerged coronavirus disease 2019/20 (COVID-19) caused by infection with the severe acute respiratory syndrome coronavirus 2 (SARS-CoV-2) has spread rapidly across the world since December 2019.[5,6] As of September 9, 2021 there have been more than 222 mio. confirmed cases and 4.5 mio. death cases globally related to COVID-19, according to the World Health Organization. Currently, although very efficient vaccines are available, the worldwide number of infections is still rapidly growing, impacting billions of people's lives not only in acute infections but also in long term perspectives as long-COVID.[7] Therefore, developing not only safe and effective vaccines but also drugs against SARS-CoV-2 is urgently needed. First of all, a number of important repurposed antiviral drugs (e.g., Lopinavir, Hydroxychloroquine, and Ritonavir)[8] have been licensed to treat COVID-19. Medicinal chemists in academia and at companies are seeking for new drugs for the treatment of infections by not only SARS-CoV-2 but also for a broad spectrum of RNA viruses.[9]

For several decades, many RNA or DNA polymerase inhibitors based on nucleoside analogs (e.g., HIV-RT and nucleos(*t*)ide reverse transcriptase inhibitors (NRTIs)) are extensively used as the backbone to combat infections caused by HIV, influenza, hepatitis B and hepatitis C virus, herpes virus and recently SARS-CoV-2.[10–15] Mainly these compounds target the virus replication by interfering with the action of the virus specific polymerases. In this respect they either act as obligate or as non-obligate chain terminators which in both cases finally lead to incomplete replication of the viral genome and thus incompetent new virus particles. A further mechanism of action of such compounds is that—if they are not repaired after incorporation—they induce a high number of mutations within the viral genome leading finally to lethal mutagenesis by error catastrophe. In order to combat COVID-19, many approved nucleoside antivirals, such as Remdesivir, Sofosbuvir, and Tenofovir have been used to combat this virus-caused pandemic (repurposing approach).[16,17] Previous studies have demonstrated that the nucleobase analog Favipiravir (6-fluoro-3-hydroxypyrazine-2-carboxamide) is an antiviral agent that inhibits the RNA-dependent RNA polymerase of many RNA viruses in animal infection models,[18,19] including Influenza virus (types A, B and C) infection,[18–22] Lassa virus infection,[23] severe fever with thrombocytopenia syndrome virus (SFTSV) infection,[24] Ebola virus (EBOV) infection,[25] Rabies virus infection,[26] Rift Valley fever virus (RVFV) infection,[27] Western equine encephalitis virus (WEEV) infection,[28] West Nile virus (WNV) infection,[29] Norovirus infection,[30] Crimean-Congo hemorrhagic

fever virus (CCHFV) infection,[31] Yellow fever virus disease (YFV) infection,[32] and Hantavirus virus (HRTV) infection.[33] Favipiravir was developed by the Japanese Toyama Chemical Company for the treatment of severe or pandemic influenza[18,21] and was first approved in Japan in 2014 to treat human influenza virus infections.[34] Recently, Favipiravir has been demonstrated to be a potential agent for COVID-19 patients.[35,36] Due to its successful antiviral potency, Favipiravir was first approved for clinical use in China in March 2020 to treat SARS-CoV-2 infections.[35,37]

The antiviral efficacy of many nucleos(*t*)ide polymerase inhibitors is strongly dependent on their intracellular activation by host cellular kinases to yield, via the nucleoside monophosphate (NMP) and nucleoside diphosphate (NDP), ultimately the bioactive nucleoside analog triphosphate (NTP). The nucleobase analog Favipiravir (T-705) first undergoes metabolic activation through phosphoribosylation to form ribofuranosyl-5′-monophosphate (Favipiravir-RMP, T-705-RMP) by the eukaryotic hypoxanthine guanine phosphoribosyltransferase (HGPRT) which is then converted through intracellular phosphorylation into its ribofuranosyl-5′-triphosphate metabolite (Favipiravir-RTP, T-705-RTP) most probably by host cell enzymes (Fig. 1).[22,38] In previous studies the ribofuranosyl-5′-diphosphate metabolite (Favipiravir-RDP, T-705-RDP) was not observed or was formed in amounts below the limit of detection. However, the enzymes involved in the conversion of T-705-RMP into T-705-RDP and T-705-RTP have not been completely identified.[22,38,39]

Earlier, Favipiravir is noted as a promising drug for the treatment of infections caused by different RNA viruses probably due to the inhibition of the RdRP by T-705-RTP in a dose-dependent manner.[18,19,22,40] However, Favipiravir is effective on SARS-CoV-2 and other RNA viruses at high doses only,[41] In addition, it was shown that Favipiravir has a risk for embryotoxicity and teratogenicity.[42] Based on these concerns, the Ministry of Health, Labor and Welfare has formulated strict regulations on its production and clinical use.[42]

Recently, the related pyrazine derivative (T-1105; 3-hydroxy-2-pyrazinecarboxamide), which is the non-fluorinated T-705 analog has also shown promising results in the treatment of influenza virus[43] and other RNA viruses. Also its nucleoside analog form T-1106 (3,4-dihydro-3-oxo-4-β-D-ribofuranosyl-2-pyrazinecarboxamide; Fig. 1) showed potent antiviral activity against RNA viruses without significant toxicity to mammalian cells.[20–22,32,44,45] As T-705, T-1105 needs activation into its triphosphorylated form but proved to be more efficiently activated by human

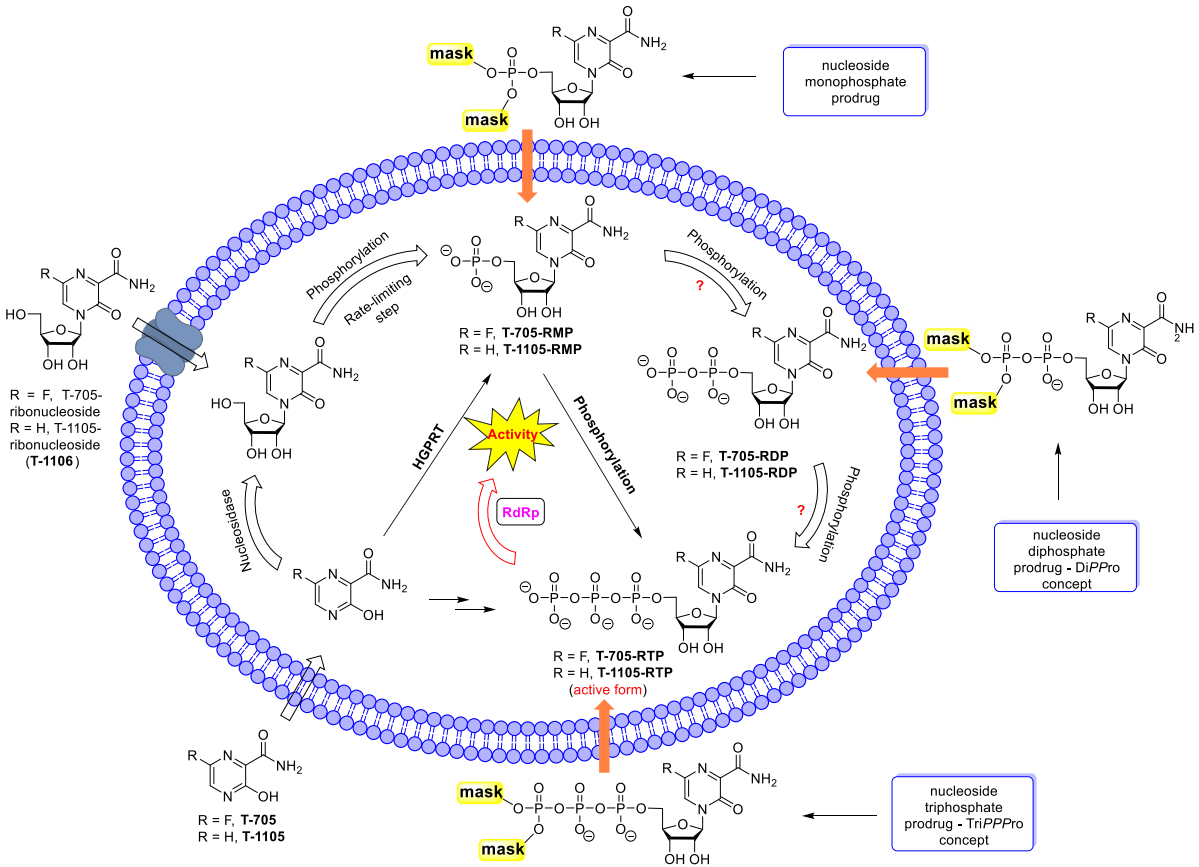

Fig. 1 Mode of action of Favipiravir (T-705) and T-1105 and the corresponding nucleoside prodrug approach.

HGPRT than T-705 in influenza virus infected MDCK cells.[39] The antiviral activity of the nucleoside analog T-1106 was in many cases virtually similar to T-705, although the dose of T-1106 required was lower than that of T-705.

Earlier studies have shown that both T-705 and T-1105 are poor substrates for the HGPRT and thus the overall conversion of T-705 and T-1105 into their corresponding nucleoside triphosphates (T-705-RTP and T-1105-RTP) has been identified as being the limiting factor for the antiviral activity.[39] So, it would be beneficial to use the already phosphorylated metabolites as potential drugs, in the extreme to use the ultimately active triphosphate of the two nucleobase analogs. However, the charged phosphorylated metabolites cannot be considered as viable drug candidates because of their high polarity which prevents cell membrane penetration. To overcome the inefficient phosphorylation of nucleoside analogs T-705 and T-1105 and thus to achieve the higher intracellular concentration of its active metabolites (T-705-RTP and T-1105-RTP), several pronucleotide strategies developed by our group, such as nucleoside monophosphate prodrugs (*cyclo*Sal), nucleoside diphosphate prodrugs (Di*PP*roconcept), and nucleoside triphosphate prodrugs (Tri*PPP*ro-concept) have been applied to the nucleoside forms of T-705 (Favipiravir) and T-1105 (T-1106; Fig. 1).[46]

This minireview summarizes the application of our mono-, di-, and triphosphate pronucleotide approaches to T-705 and T-1105 and other nucleoside analogs. The synthesis, hydrolysis properties, and structure–activity relationships in the antiviral evaluation of these prodrugs are discussed here briefly.

2. T-705/T-1105 mechanism of action (MoA)

For all positive stranded RNA viruses like influenza, Ebola and also SARS-CoV-2, RdRp's play a crucial role in the viral RNA replication. In case of SARS-CoV-2 this protein is coded nsp12. The role of nsp12 makes it an ideal target for antiviral agents due to the importance for the viral life cycle and the lack of host homologs.

Intracellular nucleoside analog 5′-triphosphates (NA-TPs) are then incorporated by error-prone viral RdRp's into the nascent viral RNA.[47–49] This can lead to a disruption of the RNA synthesis by chain termination, or can lead to lethal mutagenesis. In contrast to other RNA viruses, SARS-CoV-2 has the possibility to remove nucleoside analogs from the viral

RNA after the incorporation by nsp12, which is carried out by the RNA proof-reading exoribonuclease (nsp14-ExoN).[50] This can lead to resistance development of SARS-CoV-2 against nucleoside analogs. For example, it has been shown that nsp14 is capable of excising Ribavirin, a long-known broad-spectrum antiviral nucleoside analog, from the viral genome due to its proof-reading capabilitys.[51,52] Nevertheless several antivirally active nucleoside analogs are currently under investigation as potential anti-SARS-CoV-2 candidates.[17,53,54] Although Favipiravir is currently part of clinical trials for treatment of SARS-CoV-2, the exact MoA is still not finally determined. Several previous studies showed that the antiviral activity of T-705-RTP relies on its mutagenic properties.[55–59]

Moreover, two independent studies were published showing that the incorporation of a single or two consecutive T-705 molecules led to chain termination.[60–62] To get a deeper understanding of the MoA, in a collaborative work with the group of B. Canard, SARS-CoV-2 infected Vero cells were cultivated in the presence (500 μM) or absence of T-705.[63] Subsequently, a deep sequencing of viral RNA was performed. It could be observed, that in the presence of T-705 the total mutations are 3-fold higher and the G—A and C—U transition mutations increased by 12 times compared to the absence of T-705. The increase in mutation frequency has also a measurable antiviral effect on SARS-CoV-2. The viral replication is inhibited with an EC_{50} value of 0.2 mM and the virus-induced cytopathic effect is lowered with an EC_{50} value of 0.1 mM. In SARS-CoV-2 infected cells, the fact that T-705 has an antiviral effect showed first that T-705 manages to avoid removal from the viral RNA by nsp-14. The second conclusion that can be made is that the inhibition of the replication is, at least partially, caused by the lethal mutagenesis induced by T-705. Even more effective as the T-705-RTP was the T-1106 triphosphate analog.

To determine the exact amount of T-705 and T-1105 that are incorporated by the SARS-CoV-2 RdRp into the viral RNA, enzyme assays with the isolated RdRp were performed. These experiments should also help to get a deeper understanding of the MoA. First, the primer dependent activity of the nsp12 using annealed primer-templates (PT) and self-priming hairpin (HP) RNA's was determined. The RNA synthesis of nsp12 alone is not efficient, this result is consistent with prior studies.[64,65] For an efficient RNA synthesis, the cofactors nsp7 and 8 are essential. Together with these cofactors the nsp12 forms a four-component complex containing a nsp7/nsp8 heterodimer and a nsp8 monomer. Interestingly, the addition of further nsp8 to this nsp12:nsp7L8 complex, forming the nsp12:nsp7L8:8 complex

further increases the efficiency of the RNA synthesis, both on primer-templates (PT) and self-priming hairpin (HP) RNAs.[63] This nsp12 complex was used for elongation reactions in the presence of T-705-RTP and T-1105-RTP with simultaneously omission of ATP and/or GTP. For both, the PT and HP substrate, multiple incorporation events could be observed. However, T-705-RTP proved less efficient as compared to T-1105-RTP. The lower efficiency of T-705-RTP matches with previous results mentioned (see below) and may be explained by the lower chemical stability of T-705-RTP compared to T-1105-RTP.[66] The experiment also clearly showed that both nucleoside analogs are functioning as purine analogs as they are not incorporated in place of uracil and cytosine.

If the HP complex is used both nucleoside analogs are efficiently incorporated opposite of uracil and cytosine and the formation of full-length products can be observed. These results suggest that lethal mutagenesis is the MoA if HP was used as substrate. If on the other hand PT is used as substrate a different MoA was observed depending on whether the nucleoside analogs are incorporated opposite of uracil und cytosine. Both nucleoside analogs are rapidly incorporated opposite of uracil but further extension is slow and inefficient. Multiple consecutive incorporations even lead to complete stop of the extension. Opposite of cytosine however a marked stall in replication before each incorporation of a nucleoside analog occurred, but after incorporation the elongation proceeds rapidly. In these experiments without adding GTP more full-length products were observed. Previous studies showed for the poliovirus RdRp that these pause events before the incorporation of T-705/T-1105, opposite of cytidine, are caused by backtracking of RdRp, which was attributed the primary cause of the antiviral activity.[67] The results of this work suggest that for nsp12 the MoA of T-705/T-1105 is dictated by the structural and functional properties of the polymerase and the RNA. The proof of not fully elongated RNA strains suggests that chain termination may contribute to the antiviral effect as well as chain termination, although it is not the predominant MoA, because chain termination could only be observed after several consecutive incorporations of the nucleoside analogs. Due to the fact that consecutive incorporation is relatively unlikely and based on the speed and frequency of the incorporation of T-705/T-1105 it is more plausible that the antiviral effect of T-705/T-1105 is caused by its lethal mutagenic effect. This is also consistent with the earlier performed infectious virus experiments. It was also shown that the SARS-CoV-2 polymerase is the fastest viral RdRp known. It is determined that the SARS-CoV-2 nsp12 elongates with a frequency of 600–700

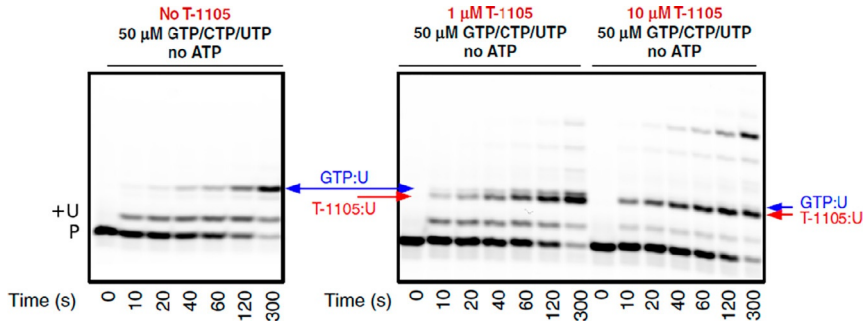

Fig. 2 Elongation reaction with the PT substrate in with each 50 μM of GTP, UTP and CTP in the absence of ATP (left) shows rapid addition of the first uracil followed by slow misincorporation of the GTP:U mismatch. If 1 μM T-1105-RTP it gets incorporated on a similar timescale as the native GTP:U mismatch (right).[63]

nucleotides per second. This is significantly faster compared to picornaviral polymerases (5–20 s^{-1}) or dengue and hepatitis C polymerase (4–18 s^{-1}).[63]

In the no-ATP experiments, GTP:U mismatches were observed, the most common naturally occurring transition mutation, allowing to compare the T-1105 incorporation rate with the appearance of the natural GTP:U transition mutation. If in the elongation reaction 50 μM GTP and 1 μM T-1105-RTP are used the T-1105:U pair occurs 5-fold more often as the GTP:U mismatch. This means that, by taking the concentration into consideration, the T-1105:U pair is by 250-fold more likely to occur then the GTP:U mismatch (Fig. 2). These huge amounts of misincorporations, compared to the natural occurring transition mutations, possibly exceed the proof-reading capacities of nsp14. Even though these results match with the infectious virus experiments, further studies have to examine if nsp14 is capable of excising T-705/T-1105, as it is the case for other nucleoside analogs, or not.[52,68,69]

3. Chemical synthesis of the nucleoside of T-705 and T-1106 as well as their monophosphates

Synthesis of T-705-RMP **3**. The polymerase assays clearly showed the huge antiviral potential of T-705/T-1105 once it gets inside the cell in their phosphorylated nucleoside forms. As described above, one limiting factor of the antiviral activity is the inefficient metabolism of T-705/T-1105 into the corresponding ribonucleoside monophophates by the human HGPRT.[39] A newer study suggests that the metabolism of the RMP into the RDP is

a second limiting bottleneck in the enzymatic activation.[39] Additionally, it was reported that the activation heavily depends on the used cell line, which makes the activation by human enzymes even more unreliable.[43] So possibly the antiviral activity could be enhanced by delivering the antiviral active metabolites directly into cells. To achieve this, one aim of our group was to develop reliable synthesis routes to prepare the T-705/T-1105-ribonucleosides which served as starting materials for the synthesis of the phosphorylated metabolites. Moreover, all these compounds then also served for applying several prodrug strategies for intracellular delivery of the corresponding nucleotides (Fig. 1).

T-705-ribonucleoside was synthesized using the Vorbrüggen-coupling method.[66] First, T-705 **1** was silylated by hexamethyldisiloxane (HMDS), the silylated base was then coupled to tetra-*O*-acetyl-β-D-ribofuranose in the presence of tin(*IV*)tetrachloride as Lewis acid. Subsequently the crude product needed to be deacetylated. Unfortunately, it was not possible to use standard deacetylation conditions using either methanolic ammonia, sodium methoxide, or a mixture of triethylamine in water and methanol, because all these conditions led to decomposition of the just formed nucleoside. This decomposition was probably due to the nucleophilicity of the reagents which are typically used in the cleavage of esters. Then, less nucleophilic reagents were used to synthesize T-705-ribonucleoside **2**. Finally, a transesterification reaction using 0.3 equivalents of dibutyltin oxide in methanol gave the desired nucleoside **2** in a yield of 40%.

Following to synthesis of the T-705-ribonucleoside the next aim was to synthesize T-705-ribonucleoside-5′-monophosphate. One of the most common method for the synthesis of 5′-monophosphates is the method of Sowa and Ouchi.[70] Using this method, a tetrachloropyrophosphate pyridinium chloride adduct was generated by adding water and pyridine to phosphorus oxychloride. The tetrachloropyrophosphate pyridinium chloride adduct then reacted with ribonucleosides selectively at the 5′-position. After hydrolysis the 5′-monophosphate was formed together with hydrochloric acid.[70] Usually this aqueous solution was then adjusted to pH 7–8 using solid ammonium carbonate to yield the monophosphate as ammonium salt. However, using these conditions led to decomposition of the T-705-RMP **3**. After modification of the reaction conditions using (i) short reaction times and hydrolysis times and (ii) careful neutralization using aqueous ammonium bicarbonate solution, it was possible to obtain the T-705-RMP **3** in a yield of 50% (Scheme 1).[66] Further studies on the chemical stability showed not only a significant stability of the glycosidic bond but also a chemical instability of the fluorinated heterocycle itself.[66]

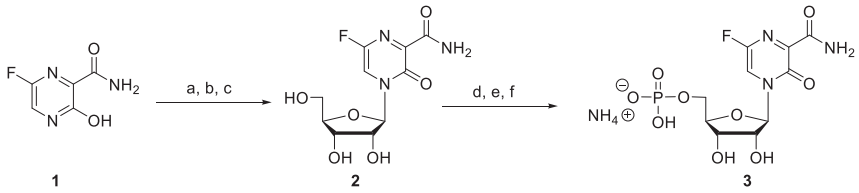

Scheme 1 Synthesis of T-705-ribonucleoside-5′-monophosphate **3**: (A) HMDS, $(NH_4)_2SO_4$, 60 min, 140°C; (B) tetra-*O*-acetyl-β-D-ribofuranose, $SnCl_4$, CH_3CN, 7 h, rt.; (C) Bu_2SnO, MeOH, 24 h, 80°C, overall yield: 40%. (D) phosphorous oxychloride, pyridine, H_2O, 30 min, 0°C. (E) addition of **2**, 20 min, 0°C. (F) ice H_2O, 30 min, aqueous saturated NH_4HCO_3 (pH 7.0), overall yield: 50%.

Synthesis of T-1106-MP **9**. Stability studies showed that T-1106 **5** proved chemically completely stable in contrast to T-705-ribonucleoside **2.**[66] Additionally, Balzarini *et al.* reported that the 3-hydroxyl function of T-705 is critical for their substrate recognition by HGPRT but that the 5-fluoro atom of T-705 is not required for metabolic activation and antiviral activity.[39] Due to these facts the synthetic focus of our group shifted away from T-705 towards T-1105.

T-1106 **5** was synthesized using the Vorbrüggen-coupling method using standard conditions; also the subsequent deacetylation under standard conditions worked without any problems and yielded the desired nucleoside **5** in a yield of 55% (Scheme 2).[66]

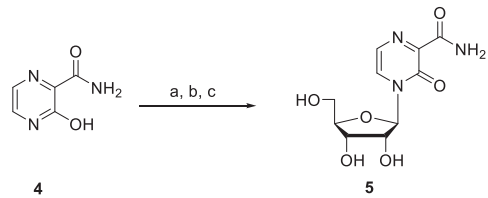

Scheme 2 Synthesis of T-1106 **5**: (A) tetra-*O*-acetyl-β-D-ribofuranose, *N,O*-bis (trimethylsilyl)acetamid, CH_3CN, 30 min, rt.; (B) trimethylsilyl trifluoromethansulfonate, CH_3CN, 44 h, rt.; (C) MeOH, H_2O, Et_3N, 6 h, rt., overall yield: 55%.

The one step phosphorylation method of Sowa and Ouchi[70] to convert T-1106 **5** into the 5′-monophosphate was not successful. Thus, an alternative route was developed to synthesize the monophosphate using phosphoramidite chemistry. First, the 5′-OH group of **5** was dimethoxytrityl (DMTr)-protected followed by the acetylation of the 2′- and 3′-OH groups. Subsequently, the DMTr group was cleaved under acidic conditions to yield compound **7** (65%). The monophosphate **9** was then synthesized using bis(9H-fluoren-9-ylmethyl)-diisopropylamino-phosphite. After basic cleavage of the *O*-acetyl

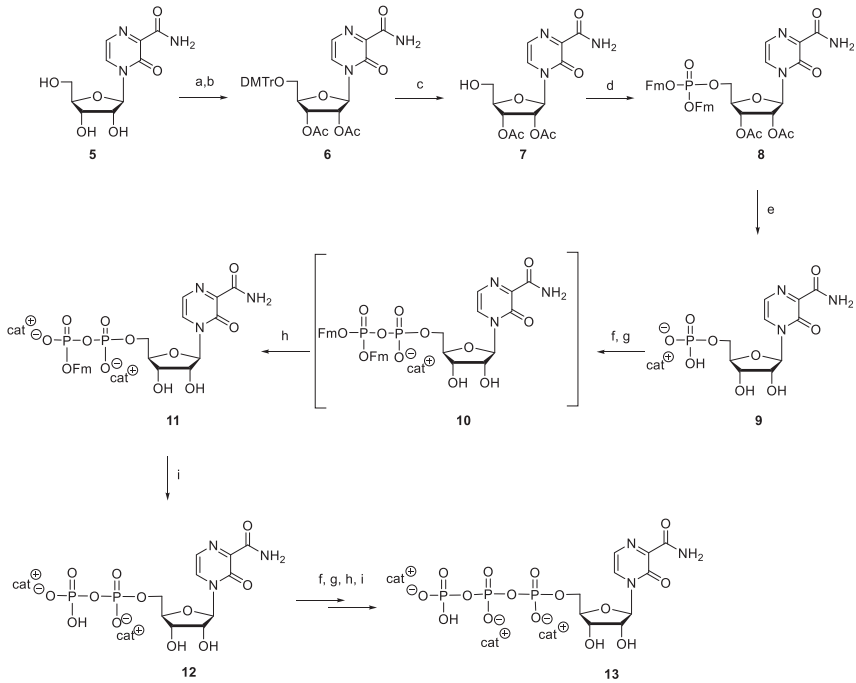

Scheme 3 Synthesis of T-1106-DP **12** and -TP **13**: (A) DMTrCl, C_5H_5N, CH_3CN, 2 h, rt.; (B) TEA, Ac_2O, C_5H_5N, CH_3CN, 16 h, rt., 75% over two steps; (C) CH_3OH, *p*-toluenesulfonic acid, 10 min, rt., 84%; (D) 1. bis(9H-fluoren-9-ylmethyl)-diisopropylaminophosphite (in CH_2Cl_2), DCI, CH_3CN, 15 min, rt.; 2. TBHP, CH_3CN, 10 min, rt.; (E) TEA, CH_3CN, 72 h, rt.; then CH_3OH/H_2O/TEA 7:3:1, 24 h, rt., 72% over steps (D–E); (F) bis(9H-fluoren-9-ylmethyl)-diisopropylamino-phosphite (in CH_2Cl_2), DCI, DMF, 10–20 min, rt.; (G) TBHP, DMF, 5 min, rt.; (H) TEA, CH_3CN, 10–20 min, rt.; (I) TEA, H_2O, CH_3CN, 24–48 h, rt.

and fluorenylmethyl groups, T-1106-MP **9** was synthesized in an overall yield of 47% (Scheme 3).[46]

Synthesis of the T-1106-DP **12** *and -TP* **13**. The T-1106-DP **12** and -TP **13** were synthesized using an iterative strategy starting from the T-1106-MP **9** (Scheme 3).[71] It was not possible to perform a purification on the double Fm-protected diphosphate **10** because it rapidly hydrolyzed during purification. A selective cleavage of one single Fm-group was achieved by the short (5–20 min) treatment of **10** with triethylamine. The isolated intermediate **11** was stable towards hydrolysis and it was possible to separate the monophosphate using RP-chromatography. After an additional deprotection step T-1106-DP **12** was obtained in high purity (>98%) in an overall yield of 53%. The triphosphate **13** was then obtained by repeating the same steps, starting from the diphosphate **12** (purity of >96%; overall yield 25%.

4. *Cyclo*saligenyl (*cyclo*Sal) nucleoside monophosphate prodrug approach

Often the first metabolic phosphorylation of nucleoside analogs into their nucleoside monophosphates (NMPs) has been identified to be the limiting step in the intracellular anabolic phosphorylation cascade. Here, the use of lipophilic NMP pronucleotides may serve as intracellular delivery system for NMPs. In an attempt to obtain a neutral, lipophilic phosphate ester various masking units have been introduced with the aim to neutralize the negative charges at the phosphate or phosphonate metabolites by compensating the hydrophobicity to ensure a cellular uptake.

In our laboratories, one of the most extensively explored type of NMP prodrug approach was developed (*cyclo*Sal-technology).[72] The *cyclo*Sal technology is based on a pH-driven chemical hydrolysis and the phosphate group of the NMP are masked by salicyl alcohols **14** (Scheme 4).

The synthesis of the *cyclo*Sal-pronucleotides has been achieved either by using P(III) or P(V) chemistry (Scheme 4). First salicyl alcohols **14** were synthesized from salicyl aldehydes or salicylic acids.[73] Cyclic saligenylchlorophosphanes **15** were prepared from diols **14** and PCl_3 in yields between 50% and 85% (Method A). Next, compounds **15** were reacted with the nucleoside analog d4T in the presence of diisopropylethylamine (DIPEA)

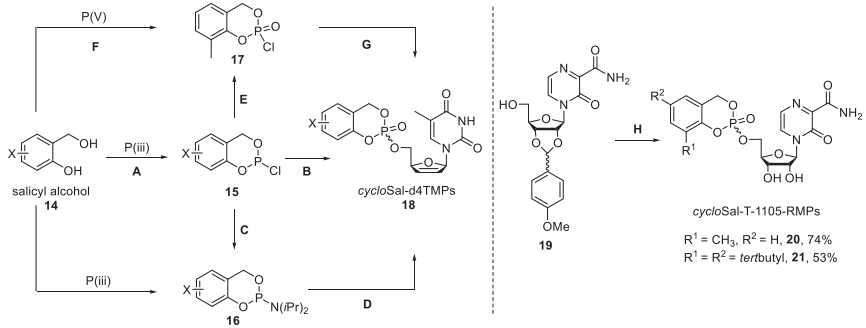

Scheme 4 Synthesis of *cyclo*Sal-d4TMP triesters **18** and T-1106-*cyclo*Sal-prodrugs **20**,**21**. Method A: PCl_3, pyridine, Et_2O, −10°C, 2 h, 50–85%; Method B: (i) d4T, DIPEA, CH_3CN, −20°C to rt., 1 h; (ii) TBHP, CH_3CN, −20°C to rt., 1 h, 50–73%; Method C: diisopropylamine, Et_2O, 0°C, 30 min, 50–85%; Method D: (i) d4T, pyridinium chloride, tetrazole or imidazolium triflate, CH_3CN, 0°C, 30 min; (ii) TBHP, CH_3CN, rt., 1 h, 70–95%; Method E: O_2, toluene, rt., 16 h, quant; Method F: $POCl_3$, TEA, CH_2Cl_2, −60°C to rt., 61%; Method G: d4T, pyridine, −50°C, 4 h, 83–95%; Method H: (i) *cyclo*Sal-phosphochloridite, TEA, CH_3CN, DMF, 15–20 min, rt.; (ii) TBHP, CH_3CN, DMF, 1–2 h, rt.; (iii) TFA, CH_2Cl_2, TFA, 1 h, rt. *Cyclo*Sal-T-1105-RMP prodrug **21** was obtained in 87% purity.

to generate cyclic phosphite triesters, followed by addition of *tert*butyl hydroperoxide (TBHP) to yield *cyclo*Sal-pronucleotides (exemplified shown here for *cyclo*Sal-d4TMPs **18**). *Cyclo*Sal-pronucleotides such as **18** were obtained as mixtures of diastereomers in reliably yields of 50–73% (Method B). Alternatively, compounds **15** were reacted with diisopropylamine to obtain phosphoramidites **16** (Method C). Then, phosphoramidites **16** were coupled to d4T in the presence of a weak acid and subsequent oxidation with TBHP (Method D). In some cases, the yields were markedly higher (up to 95%) than those obtained according to method B. Using P(V) chemistry, diols **14** were first reacted with $POCl_3$ to form 3-methyl-*cyclo*saligenylphosphorochloridate **17** (Method F).[74] The yields obtained by this method to give the *cyclo*Sal-d4TMPs **18** varied between 83% and 95%. In 2018, this technology has been also applied to T-1105 and T-705 to bypass the rate limiting formation of the phosphorylated nucleobase analog by HGRPT. C*yclo*Sal-T-1105-RMP prodrugs **20**,**21** were prepared to deliver the nucleoside monophosphate.[46]

In contrast to other NMP prodrug strategies based on enzymatic activation,[7576–84] *cyclo*Sal pronucleotides enable the intracellular delivery of the target nucleoside monophosphate by a non-enzymatically induced chemical reaction. The *cyclo*Sal-prodrugs were sensitive to basic conditions (Scheme 5).[85] The phenyl phosphate ester bond was preferably cleaved (step a) to form the benzyl phosphate diester **22**, followed by spontaneous cleavage of the benzyl ester bond (step b) releasing the NMP and salicylalcohol **14** (step b). In contrast, the alternative cleavage of the benzyl ester bond in *cyclo*Sal-d4TMP-prodrug **23** is unfavorable (step c). Furthermore, the initial hydrolysis step of these *cyclo*Sal-pronucleotides can be influenced by substituents in the 4-position of the phenol phosphate esters: electron withdrawing groups, such as nitro- or chloro-substituents, result in short half-lives. In the past, a variety of *cyclo*Sal-prodrugs with different nucleoside analogs (d4T, ddA, ddI, BVdU, and ACV) have been reported.[86–90] As expected, T-1106-*cyclo*Sal-prodrugs **20**,**21** showed a highly selective delivery of T-1105-RMP in phosphate buffer (PBS, pH 7.3) (Fig. 3).[46]

*Cyclo*Sal-phosphate triesters were evaluated for their antiviral activity in HIV-1- and HIV-2-infected wild-type CEM/0 cells and in HIV-2-infected mutant thymidine kinase-deficient CEM/TK^- cells and were compared to the parent nucleoside analogs. Most of the *cyclo*Sal-d4TMP triesters proved at least as active as d4T against HIV-1 and HIV-2 in wild-type CEM/0 cells. Moreover, some *cyclo*Sal phosphate triesters were markedly more active against HIV-2 in CEM/TK^- cells as compared to the parent d4T.[91,92] The antiviral activity of different nucleoside *cyclo*Sal-phosphate triesters

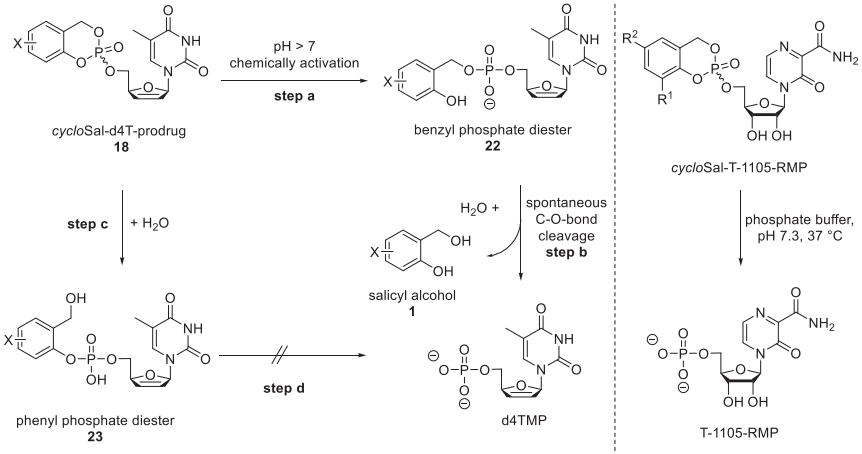

Scheme 5 Hydrolysis pathways of the *cyclo*Sal-d4TMP triesters **18** (left) [85] and T-1106-*cyclo*Sal-prodrugs **20,21** (right).[46]

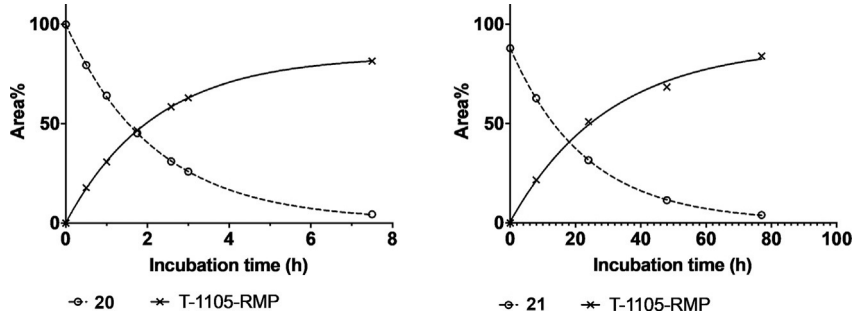

Fig. 3 Chemical hydrolysis of *cyclo*Sal-pronucleotides **20,21** in pH 7.3 phosphate buffer at 37°C.[46]

improved by the introduction of the *cyclo*Sal masks, e.g., *cyclo*Sal-ddAMP ($EC_{50} = 0.025$ μM) was 100-fold more active as the parent ddA ($EC_{50} = 4.3$ μM)[93,94] and *cyclo*Sal d4AMP was 600-fold ($EC_{50} = 0.05$ μM) more potent than d4A ($EC_{50} = 30$ μM).[88] These results proved (i) the uptake of the *cyclo*Sal-triesters into cells, (ii) the successful intracellular delivery of NMPs, and (iii) that the *cyclo*Sal-concept enables the bypass the first phosphorylation step usually needed for the initial activation of nucleoside analogs. Unexpectedly, the corresponding T-1106-*cyclo*Sal-prodrug **20** showed very poor anti-influenza virus activity (an average $EC_{50} = 248$ μM in MDCK cells and an average $EC_{50} = 232$ μM in MDCK-TG^{res} cells, Table 1), probably due to their low chemical stability ($t_{1/2} = 1.2$ h) and low lipophilicity.

Table 1 Anti-influenza virus activity and cytotoxicity in MDCK and MDCK-TG^{res} cells.[a]

Comp.[b]	MDCK cells						MDCK-TG^{res} cells					
	Cytotoxicity[c]		Antiviral activity (EC_{50} in μM)[b]				Cytotoxicity[c]		Antiviral activity (EC_{50} in μM)[b]			
	MCC	CC_{50}	A/X-31		B/Ned/537/05		MCC	CC_{50}	A/X-31		B/Ned/537/05	
			CPE	MTS	CPE	MTS			CPE	MTS	CPE	MTS
20	>400	>400	280 ± 120	>400	176 ± 42	135 ± 77	>400	>400	256 ± 39	368	200 ± 20	106 ± 47
35	21 ± 5	35 ± 8	5.4 ± 1.0	10 ± 2	7.2 ± 0.5	3.5 ± 0.6	16 ± 0	22 ± 6	6.6 ± 2.5	8.8 ± 2.4	3.4 ± 1.3	2.8 ± 1.2
36a	37 ± 3	>100	1.3 ± 0.2	1.0 ± 0.2	0.81 ± 0.05	0.56 ± 0.08	22 ± 4	44 ± 8	1.3 ± 0.2	0.97 ± 0.13	0.55 ± 0.07	0.39 ± 0.05
36b	21 ± 5	31 ± 0	1.5 ± 0.3	1.6 ± 0.3	0.67 ± 0.12	0.58 ± 0.07	16 ± 0	17 ± 1	1.5 ± 0.3	1.4 ± 0.1	0.66 ± 0.04	0.53 ± 0.17
52a	16 ± 0	30 ± 1	2.6 ± 0.0	3.6 ± 0.5	2.6 ± 0.6	2.4 ± 0.8	13 ± 3	10 ± 0	2.6 ± 0.0	4.5 ± 2.0	1.9 ± 0.3	1.0 ± 0.7
52b	16 ± 0	38 ± 5	6.0 ± 0.4	6.7 ± 2.0	9.9 ± 0.6	6.0 ± 1.9	16 ± 0	10 ± 1	5.6 ± 0.8	5.4 ± 1.3	2.6 ± 0.0	1.5
T-1105	>250	>250	6.4 ± 0.9	5.4 ± 0.6	2.8 ± 0.4	2.1 ± 0.2	>250	>250	>250	>250	>250	>250
T-705	>250	>250	24 ± 1	26 ± 2	9.0 ± 0.8	8.3 ± 1.0	>250	>250	>250	>250	>250	>250
T-1106	>250	>250	58 ± 3	52 ± 3	24 ± 2	19 ± 2	>250	>250	53 ± 4	51 ± 3	20 ± 3	19 ± 2

[a]Data are the means ± SEM of 2–5 independent tests. MDCK: Madin-Darby canine kidney cells; MDCK-TG^{res}: 6-thioguanine-resistant MDCK cell line lacking functional HGPRT.
[b]Antiviral activity is expressed as the EC_{50}, defined as the compound concentration producing 50% inhibition of virus replication, as estimated by microscopic scoring of the CPE or by measuring cell viability in the formazan-based MTS assay.
[c]Cytotoxicity is expressed as the MCC, the compound concentration producing minimal changes in cell morphology, as estimated by microscopy; or CC_{50}, 50% cytotoxic concentration estimated by MTS cell viability assay.

Although the half-lives for T-1106-*cyclo*Sal-prodrug **21** ($t_{1/2} = 16$ h) was found to be significantly higher by almost a factor of 13, again no anti-influenza virus activity was detected.[46] Because the *cyclo*Sal-pronucleotide system gave nice improvements in antiviral activity and the cleavage proceeded selectively to yield the monophosphates, the failure of by-passing the enzyme responsible for the ribophosphorylation of T-1105 may also point to a further bottleneck in the activation leading to the triphosphate: the conversion of the monophosphate analog into its diphosphate derivative. This might be an explanation, why the delivery of T-1105-RMP was not sufficient to improve the antiviral activity.

5. Nucleoside diphosphate prodrugs

Despite these obvious advantages, not in all cases the *cyclo*Sal-technology was successful. As just mentioned above, T-1105 *cyclo*Sal-pronucleotides **20**,**21** showed no or very poor antiviral activity in MDCK and MDCK-TG^{res} cells.

The same happened when 3′-deoxy-3′-azidothymidine (AZT) was used.[95–97] Here, the *cyclo*Sal-approach failed to improve the antiviral activity in thymidine kinase-deficient cells.[97] One reason might be a rapid dephosphorylation of AZTMP by 3′,5′-(deoxy)nucleotidase present in the cells.[98,99] More importantly, in the metabolism of AZT, not the formation of the monophosphate derivative (AZTMP) is critical but the formation of the corresponding nucleoside diphosphate AZTDP by the host cell enzyme thymidylate kinase (TMPK).[100,101] Consequently, it was expected that the development of nucleoside diphosphate prodrug systems would help to overcome these problems.

Earlier, very few approaches have been developed for nucleoside diphosphate prodrugs, probably because of the inherent instability of the phosphate anhydride bond. In 1990, Hostetler *et al.* designed several potential NDP-diglyceride prodrugs.[102–105] This approach was successfully used for different nucleosides and improved antiviral activities compared to the parent nucleosides, e.g., for 3′-deoxythymidine (3dT, up to 37-fold). Later, Huynh-Dinh *et al.* developed the acylphosphate concept based on a selective cleavage of these mixed anhydrides releasing NDPs in aqueous buffer.[106–108] However, in contrast to the NDP-diglyceride approach, no improvement of the antiviral activity was detected as compared to the parent nucleoside.

In order to improve the stability of the masked pyrophosphate unit, we decided to design a pronucleotide approach based on masking the negatively charged β-phosphate group only, namely, the Di*PP*ro-approach.

5.1 Nucleoside diphosphate prodrugs based on *cyclo*Sal-approach

Initially the previously developed *cyclo*Sal-technology was applied to AZTDP, (*cyclo*Sal-AZTDP prodrugs **24**; Scheme 6, upper section). The nucleoside monophosphate was prepared from AZT by the Sowa–Ouchi method.[70] After the coupling reaction of *cyclo*Sal-phosphorochloridate **17** (P(V)-reagent) and AZTMP, *cyclo*Sal-AZTDP prodrugs **24** were prepared using phosphorochloride chemistry. It was expected that such a construct would allow a rapid conversion of the Di*PP*ro-AZT prodrugs **24** into AZTDP. The *cyclo*Sal-AZTDPs **24** were incubated in PBS (pH 7.3) to study their chemical stability and to identify the formed hydrolysis products. To our surprise, only a very small amount of AZTDP (1%, Scheme 6, pathway a) but a predominate formation of AZTMP (99%, Scheme 6, pathway b) was detected in these studies. The undesired pyrophosphate cleavage leading to AZTMP and *cyclo*Sal-phosphate were caused by nucleophiles attacking the β-phosphate group. Consequently, the *cyclo*Sal-principle is unsuitable to bypass the second intracellular phosphorylation step.

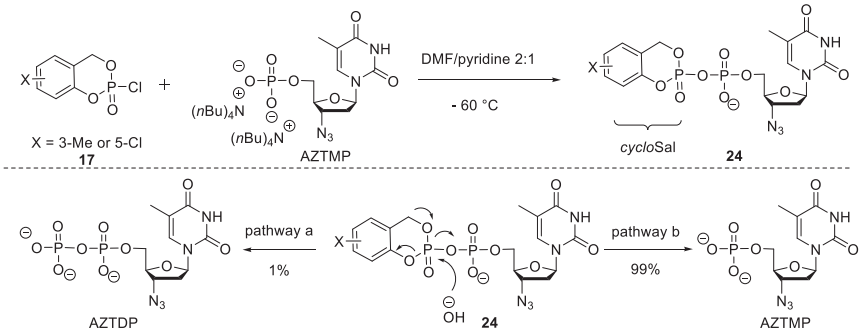

Scheme 6 Synthesis and hydrolysis of *cyclo*Sal-AZTDPs **24**.

5.2 The symmetric Di*PP*ro-nucleoside diphosphate prodrugs

Guided by the results from *cyclo*Sal-AZTDP prodrugs **24**, we aimed to design a new approach based on an enzymatically triggered pronucleotide delivery system[109] that has two masking groups at the β-phosphate. In 2008, we reported on the synthesis of the first examples of the bioreversible

protection of nucleoside diphosphates using the phosphoramidite chemistry.[110] The cleavage of the phenyl ester moiety within the masking units was induced by chemical or enzymatic means to form NDP in CEM cell extracts. Later, we developed a series of Di*PP*ro-d4TDPs **28** bearing different lipophilic acyl chain lengths to study their hydrolysis properties in chemical or biological media and described structure–activity relationships in the antiviral evalution.[111–115] The synthesis of Di*PP*ro-d4TDPs **28** is summarized in Scheme 7. The method was applied to different nucleoside analogs (e.g., AZT, d4U, *carba*-isoddA) and the overall yields varied between 10% and 72%.[110–113,115]

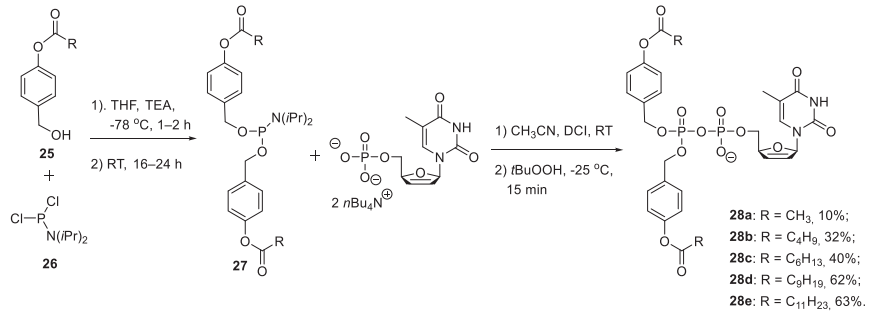

Scheme 7 Synthesis of the Di*PP*ro-d4TDPs **28**.

For the synthesis, the required nucleoside monophosphates were prepared from the nucleoside analogs as described before.[70] In contrast to the synthesis of *cyclo*Sal-nucleoside diphosphate prodrugs **24**, first bis(tetra-*n*-butylammonium)nucleoside monophosphates were coupled with a reactive P(III)-reagent comprising the lipophilic bis(acyloxybenzyl) groups to form P(III)–P(V) intermediates. Subsequently, the intermediates were oxidized with *tert*-butylhydroperoxide (TBHP) to form the corresponding diphosphates. As shown in Scheme 7, bis(4-acyloxylbenzyl)phosphoramidites **27** were prepared from benzyl alcohols **25** and (*N*,*N*-diisopropyl)dichlorophosphine **26** at low temperatures. Purified Di*PP*ro-d4TDPs **28** were obtained as brown syrups by reversed-phase (rp) column chromatography. It should be noted that the reaction could be easily followed by RP-HPLC: i) NMP was completely consumed, ii) the P(III)–P(V) intermediates were formed within few minutes and then converted to give the products.[111]

Stability studies. The Di*PP*ro-d4TDPs **28** were investigated in PBS (pH 7.3) and CEM cell extracts to study their chemical and biological stability,

respectively, and more importantly to study the delivery of the corresponding d4TDPs. Two hydrolysis pathways of Di*PP*ro-d4TDPs **28** were proposed (Scheme 8).

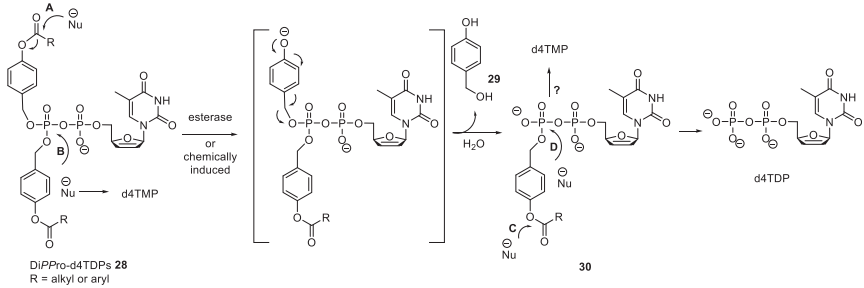

Scheme 8 Hydrolysis mechanism of Di*PP*ro-d4TDPs **28**.

In the case of Di*PP*ro-d4TDPs **28** in PBS, the chemical stability increased with the increase of the alkyl chain lengths attached to the 4-acceptor-substituted benzyl esters. The half-lives of Di*PP*ro-d4TDPs **28** were found to be between 10 h and 100 h, indicating that Di*PP*ro-d4TDPs **28** seem to be quite stable under chemical hydrolysis condition. In PBS, the starting compounds **28** disappeared and the expected mono-masked intermediates **30** were detected (Scheme 8; pathway **A**). In these studies, the ester (acceptor unit) group is converted into a strong donor hydroxy group, thus a spontaneous cleavage of the benzyl-C-O-bond occurred subsequently, leading to the formation of intermediates **30**. The half-lives of intermediates **30** (280–1400 h) were found to be much higher than for starting compounds **28**, potentially caused by repulsive interaction between the two negative charges of the intermediates and the incoming nucleophiles. Additionally, when Di*PP*ro-d4TDPs **28** were almost consumed, an increase of the d4TDP concentration and a small amount of d4TMP were observed in these studies indicating that the hydrolysis of compounds **30** mainly followed pathway **C**. Furthermore, d4TMP concentrations increased at the beginning of the hydrolytic process, probably due to the anhydride bond breakage between the α-phosphate and β-phosphate (Scheme 8; pathway **B**).

Di*PP*ro-d4TDPs **28** were investigated in human $CD4^+$ T-lymphocyte CEM cell extracts *to identify the hydrolysis products*. *The half-lives of* Di*PP*ro-d4TDPs **28** were in the range of 0.05–21 h and found to be markedly lower than the half-lives of prodrugs measured in PBS (up to 200-fold),

which indicates an enzymatic hydrolysis reaction. In the case of Di*PP*ro-d4TDPs **28**, the cleavage and the formation of intermediates **30** were observed. Former studies have shown that intermediates **30** were readily cleaved and hydrolyzed in CEM cell extracts, thus a predominate formation of d4TDP was observed and no further increase of compounds **30** concentrations were detected. It was impossible to quantify the concentrations of d4TDP released in CEM cell extracts because this compound was further dephosphorylated by enzymes, such as phosphatases, to form d4TMP.

Di*PP*ro-d4TDPs **28** were investigated for their antiviral activity in HIV-1 and HIV-2-infected wild-type CEM/0 and in HIV-2-infected mutant thymidine-kinase-deficient cells (CEM/TK$^-$). The parent d4T was used as reference compound. D4T showed no antiviral activity in thymidine kinase (TK)-deficient cells, because the first phosphorylation step to yield the monophosphate metabolite catalyzed by TK is the metabolism-limiting step. Most of the Di*PP*ro-d4TDPs **28** showed similar activities against HIV-1 and HIV-2 than the parent d4T in wild-type (CEM/0) cell cultures. In contrast, all Di*PP*ro-d4TDP prodrugs **28** were highly active in CEM/TK$^-$ cell cultures. The antiviral activity determined for prodrugs **28a–d** (AB:C1-C9) increased with increasing alkyl chain lengths due to their advantageous permeability. Di*PP*ro-d4TDP **28d** (AB-C9) was the most active compound of all the reported prodrugs: The inhibition of HIV-1 and HIV-2 replication by Di*PP*ro-d4TDP **28d** ($EC_{50} = 0.08$ μM/HIV-1; $EC_{50} = 0.32$ μM/HIV-2) improved by 11-fold and 7-fold, respectively as compared to nucleoside d4T in wild-type (CEM/0) cells and the activity was improved 1570-fold in CEM/TK$^-$ cell cultures. The antiviral activity observed in the wild-type (CEM/0) cell cultures **28d** ($EC_{50} = 0.32$ μM/HIV-2) was completely retained in CEM/TK$^-$ cell cultures ($EC_{50} = 0.11$ μM/HIV-2). It was concluded that these Di*PP*ro-prodrugs **28** were successfully taken-up across the cell membranes and delivered phosphorylated metabolites, most probably d4TDPs.

5.3 Non-symmetric Di*PP*ro-nucleoside diphosphate prodrugs

Taking all previous results into account, we next developed a second generation of Di*PP*ro-NDP compounds as shown in compounds **34** (Scheme 9). The second generation compounds comprised two *different* acyloxybenzyl moieties linked to the β-phosphate of the nucleoside diphosphate. One of the bioreversible groups is bearing a short alkyl chain

carboxylic acid ester (low lipophilicity) while the second group comprises a long alkyl residue carboxylic acid ester or a substituted benzoic acid ester (high lipophilicity). It was expected that such a design would allow a rapid conversion of the Di*PP*ro-compounds **34** into the mono-masked intermediates **30** and therefore avoid the unwanted phosphoanhydride bond hydrolysis in the prodrugs leading to NMP. The second masking unit would be subsequently cleaved slowly to form the NDP. We expected that such a design would achieve a highly selective conversion of the Di*PP*ro-prodrugs into nucleoside diphosphates.

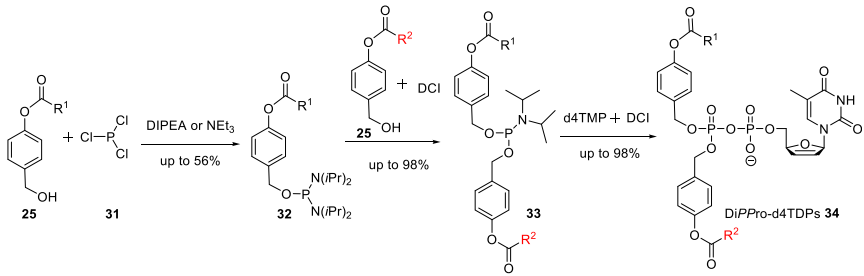

Scheme 9 Synthesis of non-symmetric Di*PP*ro-nucleoside diphosphates **34**.

Di*PP*ro-d4TDPs **34** were made according to the phosphoramidite route as summarized above.[110,112,115] First, bis(di*iso*propylamino)phosphoramidites **32** were prepared from 4-acyloxybenzyl alcohols **25** and phosphorus trichloride **31** in the presence of *N*,*N*-di*iso*propylamine (DIPA). Then, compounds **32** were reacted with the second 4-acyloxybenzyl alcohols **25** to form non-symmetric phosphoramidites **33**. Finally, phosphoramidites **33** were coupled with d4TMP in an acid-activated reaction followed by oxidation (Scheme 9).

Di*PP*ro-d4TDPs **34** were studied with regard to their stabilities in different media and their hydrolysis products were analyzed. Interestingly, in all cases, both intermediates **30a** (short acyl residues) and intermediates **30b** (long acyl residues) were formed, indicating that both masking groups of Di*PP*ro-d4TDPs **34** were involved in the hydrolysis (pathways **A** and **B**; Scheme 10). From analyzing the amounts of the formed products (intermediates **30**, d4TDP, and d4TMP) the following conclusions can be taken: (i) Di*PP*ro-d4TDPs **34** were found to be more readily cleaved to form intermediates **30b**, (ii) the intermediates **30b** bearing long alkanoyl ester moieties proved to be more stable than intermediates **30a** bearing short alkyl moieties, and (iii) an increase of d4TDP concentration and a very small amount of

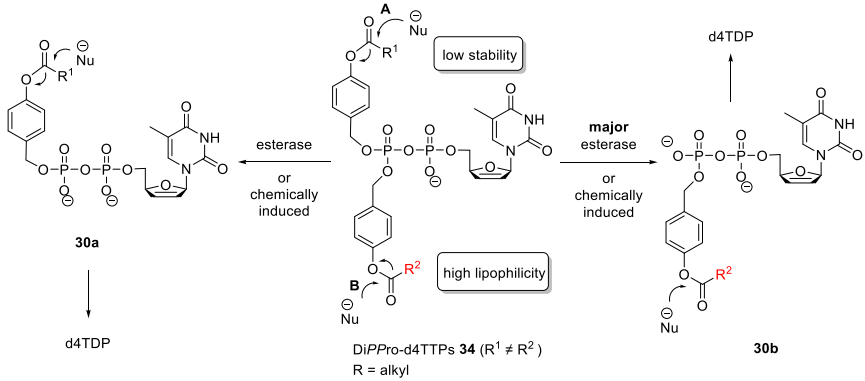

Scheme 10 Hydrolysis pathways of non-symmetric Di*PP*ro-d4TDPs **34**.

d4TMP were detected. Furthermore, the chemical stability of Di*PP*ro-d4TDPs **34** was found to be higher as compared to those of the symmetric Di*PP*ro-d4TDPs **28**. For example, the half-lives for Di*PP*ro-d4TDPs **34** (acyloxybenzyl (AB)-C1;AB-C9) ($t_{1/2} = 40$ h)[113] improved by 4-fold compared to **34a** (AB-C1;AB-C1) ($t_{1/2} = 10$ h).[110]

We evaluated the stability of Di*PP*ro-d4TDPs **34** in CEM cell extracts as well. As expected, the stability of Di*PP*ro-d4TDPs **34** in cell extracts ($t_{1/2} = 0.03$–1.91 h) was significantly lower than the stability in PBS (up to 1450-fold). The masking groups in Di*PP*ro-d4TDPs **34** were selectively cleaved to form intermediates **30a** and intermediates **30b**, respectively. In the case of Di*PP*ro-d4TDPs **34** (AB:C4;AB:R^2), the formation of the C_4H_9-intermediate and the long alkyl chain acyl group (R^2) intermediates were detected. However, for Di*PP*ro-d4TDPs **34** (AB-C1;AB-R^2), a highly selective cleavage of the short biodegradable moiety (AB:C1) led to the formation of intermediates **30b** (AB:R^2) in cell extracts. Di*PP*ro-d4TDPs **34** were also rapidly hydrolyzed by PLE and delivered d4TDP within a few minutes (0.14–0.19 min). However, for Di*PP*ro-d4TDP **34** (AB-C1;AB-C9), both alkanoyl esters were cleaved at almost identical rates. In contrast, a large amount of C_4H_9-intermediate was observed in the hydrolysis of Di*PP*ro-d4TDP **34** (AB-C4;AB-C9) with PLE.

In antiviral assays, the inhibition of the replication of HIV-1 and HIV-2 by Di*PP*ro-d4TDPs **34** was similar, or slightly better, compared to their parent nucleoside d4T in wild-type CEM/0 cells. In some cases, the antiviral activity for Di*PP*ro-d4TDPs **34** increased with the higher lipophilicity associated with the introduced masking units of the Di*PP*ro-prodrugs. The high antiviral activity of Di*PP*ro-d4TDP **34** (AB-C4;AB-C11)

($EC_{50} = 0.13\ \mu M$) was retained in thymidine-deficient CEM cells (TK^-) and compared to the parent nucleoside d4T ($EC_{50} = 150\ \mu M$) the anti-HIV activity was improved by 1153-fold.

5.4 Nucleoside diphosphate prodrugs: T-1106-Di*PP*ro-prodrugs

We applied the bis(acyloxybenzyl)-masking approach to nucleoside analogs T-705 and T-1106.[46] Starting from T-705-RMP and T-1105-RMP, T-705-Di*PP*ro-prodrug **35** ($R^1 \neq R^2$) and T-1106-Di*PP*ro-prodrugs **36** ($R^1 = R^2$ and $R^1 \neq R^2$) were successfully prepared using the previously reported phosphoramidite protocol, respectively.[110,113] The cleavage of Di*PP*ro-prodrugs **35**,**36** was further investigated in PBS (pH 7.3), with PLE (PBS, pH 7.3), and in MDCK cell extracts.

In PBS (pH 7.3), T-705-Di*PP*ro-compound **35** (AB-C4;AB-C14) was fully decomposed after 30 h. However, the expected intermediates were *not* observed. We assumed that the nucleophilic displacement of the fluorine atom by water took place which led finally to the destruction of the nucleobase analog. Furthermore, T-705-Di*PP*ro-compound **35** (AB-C4; AB-C14) was rapidly hydrolyzed with PLE and delivered the expected T-705-intermediates (with R either C_4H_9 or $C_{14}H_{29}$) much faster compared to the chemical hydrolysis. Compared to its T-705 counterpart, T-1106-Di*PP*ro-prodrugs **36** (for example **36a**, $t_{1/2} = 30$ h) showed much higher chemical stability. The chemical hydrolysis of T-1106-Di*PP*ro-prodrug **36a** (AB-C9;AB-C9) released mono-masked T-1106-intermediate **37** (AB-C9), T-1105-RDP, and T-1105-RMP (Fig. 4A, condition *without* esterase). With PLE, almost no formation of T-1105-RMP and the unknown by-product was observed. The starting material disappeared and the mono-masked T-1106-intermediate **37** (AB-C9) was formed. Subsequently, T-1106-intermediate **37** (AB-C9) was fully converted into the final metabolite, T-1105-RDP (Fig. 4A, condition *with* esterase). Furthermore, T-1106-Di*PP*ro-prodrugs **36a**,**b** were efficiently converted into the corresponding mono-masked intermediates **37** in extracts from MDCK and MDCK TG^{res} cells. Subsequently, T-1105-RDP was also detected as intermediate metabolite that was further dephosphorylated to T-1105-RMP (Fig. 5). T-1106-Di*PP*ro-prodrugs **36a**,**b** activation and release of T-1105-RDP was found to proceed faster for symmetrically masked T-1106-Di*PP*ro-compound **36a** (AB-C9;AB-C9) than for the non-symmetrically masked T-1106-Di*PP*ro-compound **36b** (AB-C4; AB-C14).

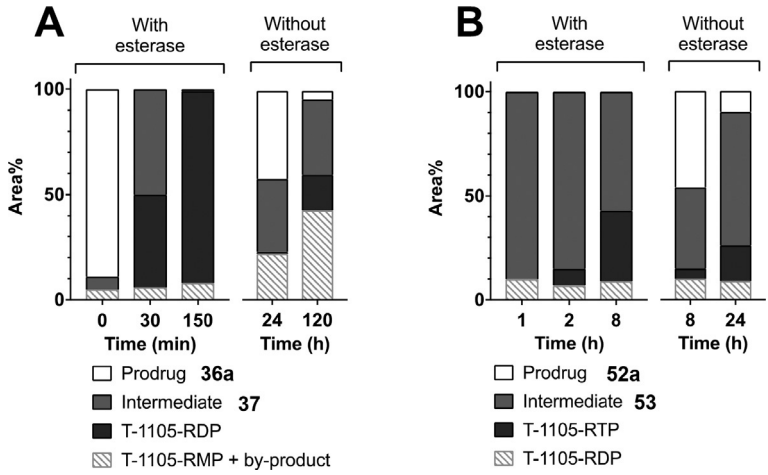

Fig. 4 Metabolic profiles of T-1106-Di*PP*ro-prodrug **36a** (A) and T-1106-Tri*PPP*ro-compound **52a** (B). T-1106-prodrugs **36a** (**A**) and **52a** (**B**) were incubated at 450 μM in the absence or presence of PLE (3 U per mL).[46]

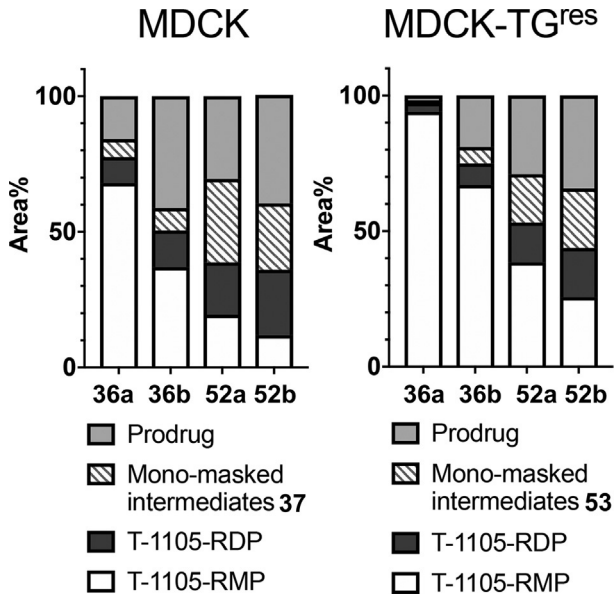

Fig. 5 Metabolic conversion of T-1106-Di*PP*ro-prodrugs **36** and T-1106-Tri*PPP*ro-prodrugs **52** in MDCK and MDCK-TG^{res} cell extracts. Prodrugs **36**,**52** (500 μM) were incubated in cell extract and after 2 h, proteins were precipitated.[46]

As expected, the initial cleavage step of the hydrolysis mechanism happened similarly to the cleavage pathways for compounds **28**,**34**, respectively. The hydrolysis pathways are shown in Scheme 11. The studies showed that: (i) a minor pathway involved the cleavage of the phosphoanhydride bond in T-1106-Di*PP*ro-prodrugs **36**, leading to T-1105-RMP, (ii) the major pathway involved an enzymatic trigger mechanism leading to T-1105-RDP via a mono-masked intermediate **37**, and (iii) with PLE, a large amount of T-1105-RDP and almost no T-1105-RMP was detected.[46]

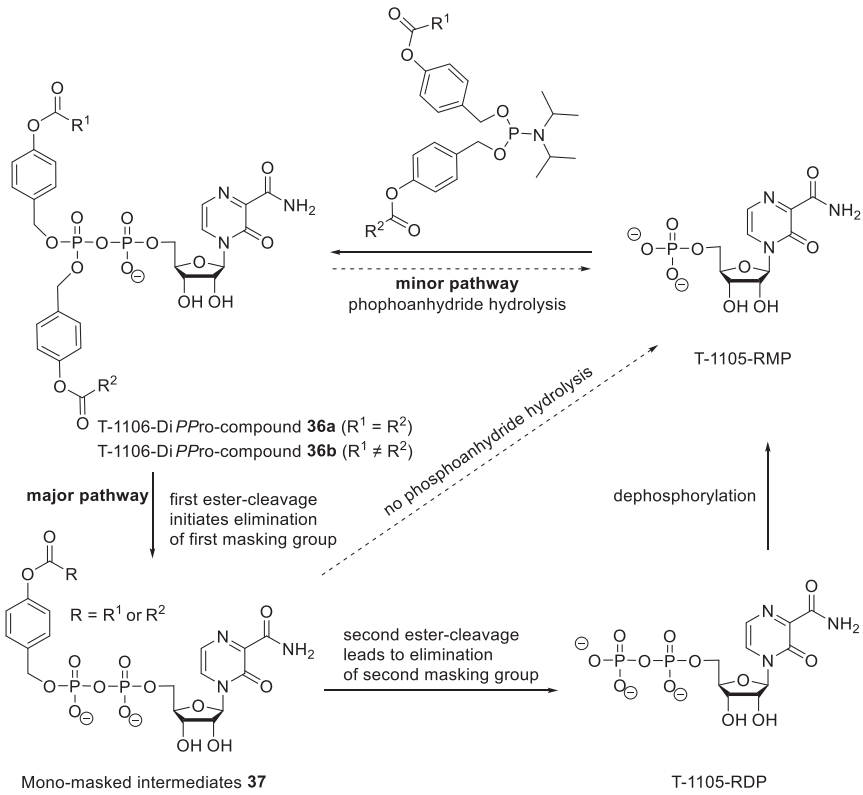

Scheme 11 Synthesis and hydrolysis mechanism of T-1106-Di*PP*ro-prodrugs **36**.

T-705-Di*PP*ro-prodrug **35** and T-1106-Di*PP*ro-prodrugs **36** were evaluated for their anti-influenza activity in MDCK and MDCK-T^{Gres} cells. As shown in Table 1, T-705-Di*PP*ro-compound **35** (AB-C4;AB-C14) had an average EC_{50} of 6.5 μM, which is 3-fold more active than the nucleobase T-705 (an average $EC_{50} = 16.8$ μM). As for T-1105 ribonucleoside

(T-1106), the anti-influenza activity of the T-1106-Di*PP*ro-prodrugs **36a**,**b** was 35 to 42-fold higher as compared to the parent nucleoside T-1106 (an average $EC_{50} = 38.2$ μM), 4 to 5-fold higher than the nucleobase T-1105 (an average $EC_{50} = 4.3$ μM), and 6 to 7-fold higher than its T-705 counterpart **35** (AB-C4;AB-C14), respectively.

Compared to the non-symmetric T-1106-Di*PP*ro-compound **36b** (AB-C4;AB-C14) ($EC_{50} = 1.1$ μM), the symmetric T-1106-Di*PP*ro-compound **36a** (AB-C9;AB-C9) had similar (an average $EC_{50} =$ 0.91 μM) anti-influenza activity. More importantly, the antiviral activity observed in MDCK-TG^{res} cell cultures (an average $EC_{50} = 0.91$ μM) was completely retained in the case of the lipophilic T-1106-Di*PP*ro-compound **36a** (AB-C9;AB-C9) in HGPRT-deficient MDCK-TG^{res} cell cultures (an average $EC_{50} = 0.8$ μM), whereas T-1106 lacked any relevant anti-influenza activity ($EC_{50} > 250$ μM). In antiviral assays, good anti-influenza activity of the T-1106-Di*PP*ro-prodrugs **36a** (AB-C9;AB-C9),**36b** (AB-C4; AB-C14) was observed in MDCK-TG^{res} cells with 5 to 7-fold improved activity as compared to the T-705-Di*PP*ro-compound **35** (AB-C4; AB-C14). Thus, T-1106-Di*PP*ro-compounds **36** provided a successful and selective delivery of T-1105-RDP inside cells and improved the anti-influenza activity and this Di*PP*ro-system proved to be highly successful in the esterase-triggered release of T-1105-RDP. As for T-705, the anti-influenza activity of T-705-Di*PP*ro-compound **35** (an average EC_{50} of 6.5 μM, 6-fold less active than T-1106-Di*PP*ro-compound **36b**) is probably limited by the chemical instability of its fluorinated nucleobase.

6. Nucleoside triphosphate prodrugs

As summarized above, we have developed a concept to deliver NDPs inside cells using lipophilic but still partially charged Di*PP*ro-compounds.[110–115] However, the released NDPs still need further intracellular phosphorylation into their antivirally active triphosphate forms by cellular kinases to interact with viral polymerases. Moreover, it was reported that even the last phosphorylation might be problematic, e.g., the conversion of FTC-DP to form FTC-TP by NDPK.[116] As a consequence, the development of nucleoside triphosphate (NTP) prodrugs is still highly interesting and desirable because this enables: i) the bypass of *all* steps of the intracellular phosphorylation and ii) the delivery of NTPs would in principle maximize the intracellular concentration of the NTPs.

In an attempt to develop NTP prodrugs, the following challenges have to solved: (i) the highly negatively charged triphosphate unit requires appropriate masking, (ii) *two* reactive phosphate anhydrides linkages in the triphosphate moieties should be kept intact, (iii) the high sensitivity for enzymatic dephosphorylation of NTPs should be prevented, and (iv) a suitable chemical synthesis has to be established. Only very few NTP prodrugs have been reported in the past.[117,118] These nucleoside triphosphate prodrugs involved the attachment of only an alkyl or acyl moiety (high lipophilicity) to the γ-phosphate moiety.[109,117–121] Unfortunately, no increase of antiviral activity was observed with these nucleoside triphosphate prodrugs as compared to their parent nucleosides.[121]

6.1 Symmetric Tri*PPP*ro-compounds—Acyloxybenzyl (AB)-nucleoside triphosphate prodrugs

Our group is working intensively on the development of NTP prodrug systems. Encouraged by the positive results of the Di*PP*ro-prodrugs, we developed a novel nucleoside triphosphate prodrug concept in which two biodegradable masking units were attached to the γ-phosphate moiety, namely the Tri*PPP*ro-approach (Scheme 12; upper section).[122] Later, we report on the application of the Tri*PPP*ro-concept on several nucleoside analogs to demonstrate the strength of the strategy (Scheme 12; lower section).[123] For the synthesis of Tri*PPP*ro-prodrugs **38**, we developed two different synthesis routes: the phosphoramidite route and the *H*-phosphonate route.[122,123]

In the initial studies, Tri*PPP*ro-d4TTPs **38** bearing two biodegradable masking groups (alkyl, alkoxyl, and aminoalkyl chains) attached to the γ-phosphate group of d4TTP were prepared using the phosphoramidite route with modest to good chemical yields (26–70%). The P(III) chemistry was similar to our previously reported phosphoramidite chemistry used for the synthesis of Di*PP*ro-prodrugs.[110,112] The difference was that the P(III)-compounds **27** were reacted with d4TDP instead of d4TMP, as the nucleotide components. For this, phosphoramidites **27** were prepared in high yields.[110,112] D4TDP was synthesized using the *cyclo*Sal-technique (55% yield). Then, compounds **27** were mixed with d4TDP in the presence of dicyanoimidazol (DCI). After oxidation, the target products were purified by automated column RP-18 chromatography.

Additionally, a further method (*H*-phosphonate route) was developed. The chemistry was based on a coupling reaction of pyrophosphate **41** (P(V)-reagent) and NMPs. *H*-Phosphonate **40** was easily prepared from

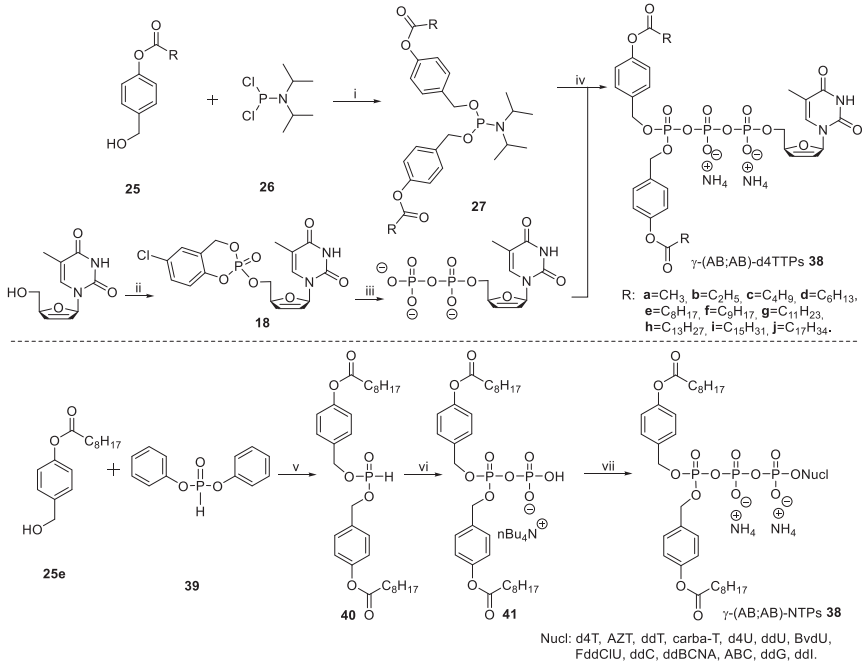

Scheme 12 Synthesis of Tri*PPP*ro-prodrugs **38** using via P(III) and P(V) chemistry. (i) Triethylamine, THF, 0 C-rt, 20 h; (ii) 1. 5-chlorosaligenylchlorophosphite, *N*,*N*-diisopropylethylamine, CH_3CN, −20 C-rt, 3 h, 2. *t*-BuOOH in *n*-decane, 0 C-rt, 30 min; (iii) $(H_2PO_4)Bu_4N$, DMF, rt., 20 h; (iv) 1. DCI, CH_3CN, rt., 1 min, 2. *t*-BuOOH in *n*-decane, 0 C-rt,15 min; (v) pyridine, 38°C, 2 h; (vi) 1. NCS, CH_3CN, rt., 2 h, 2. (H_2PO_4) Bu_4N, CH_3CN, rt., 1 h (vii) 1. TFAA, Et_3N, CH_3CN, 0 C, 10 min, 2. 1-methylimidazole, Et_3N, CH_3CN, 0 C-rt, 10 min, 3. NMP, rt., 1–3 h.

4-acyloxybenzyl alcohol **25e** and diphenyl hydrogen phosphonate (DPP) **39**. The *H*-phosphonate **40** was reacted with *N*-chlorosuccinimide (NCS) to generate a phosphorochloridate which was then reacted with tetra-*n*-butylammonium phosphate to yield pyrophosphate **41** in almost quantitative yields. Due to its high chemical instability, compound **41** was quickly purified by extraction (CH_2Cl_2/H_2O) and immediately used in the next step. Finally, compound **41** was activated with trifluoroacetic acid anhydride (TFAA) and *N*-methylimidazole,[124,125] then reacted with NMPs to give Tri*PPP*ro-NTPs **38** (*n*-Bu_4N^+ form). The target Tri*PPP*ro-NTPs **38** (NH_4^+ form) were obtained in yields between 7% and 71% using the above separation method. As compared to the phosphoramidite pathway, the *H*-phosphonate route offers some advantages: (i) NMPs are generally easier to prepare as the corresponding NDPs,

(ii) the diphosphate bond between the α- and β-phosphates was formed without oxidation step, (iii) the method was more tolerant to the used solvents, and (iv) the chemical stability of compound **40** was higher than that of the phosphoramidites **27**.

In order to study the hydrolysis properties and the delivery mechanism of Tri*PPP*ro-compounds **38**, the mono-masked acyloxybenzyl (AB)-NTP derivatives **43** were synthesized as well (Scheme 13). First, 4-acyloxybenzyl alcohols **25** reacted with 5-nitrosaligenylchlorophosphite **15** to synthesis benzyl-(5-nitro-*cyclo*Sal)-phosphate triesters **42** in high yields (up to 89%). Then, the mono-masked triphosphates **43** were prepared from 5-nitro-*cyclo*Sal-triesters **42** and d4TDP in yields of 26–30%.

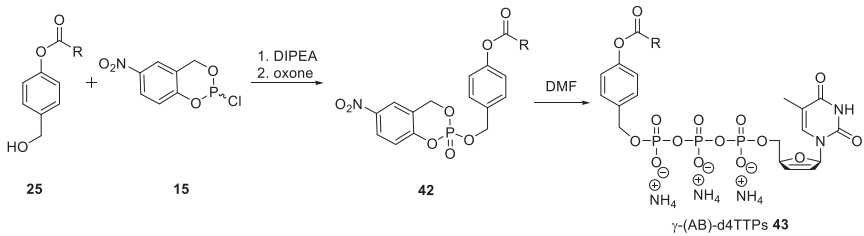

Scheme 13 Synthesis of mono-masked NTPs **43**.

In PBS, generally the half-lives of γ-(AB;AB)-d4TTPs **38a-h** increased with increasing acyl chain lengths (AB:C1-C13). Tri*PPP*ro-d4TTPs **38** hydrolyzed following similar cleavage pathways as described for Di*PP*ro-d4TDPs **28** (Scheme 8). In all cases to some extent, d4TDP was formed as well and a very low amount of d4TMP was observed in addition to the expected predominate formation of γ-(AB)-d4TTPs **43** and d4TTP, indicating that Tri*PPP*ro-d4TTPs **38** hydrolyzed mainly followed pathway **A** (**A**$^{\mathbf{1}}$ and **A**$^{\mathbf{2}}$; Scheme 14).

Furthermore, after complete conversion of the starting Tri*PPP*ro-d4TTPs **38**, no further increase of amounts of d4TDP and d4TMP was observed. It was concluded that d4TDP and d4TMP were formed from Tri*PPP*ro-d4TTPs **38** by a nucleophilic attack at the γ-phosphate (pathway **B**) or β-phosphate (pathway **C**) moiety, respectively. As observed for Di*PP*ro-d4TDPs **28**,[112] the stability of the intermediately formed γ-(AB)-d4TTPs **43** ($t_{1/2}$ = 95–637 h)[122] was higher than the corresponding Tri*PPP*ro-d4TTPs **38** ($t_{1/2}$ = 17–99 h),[122] which was in agreement with the results obtained from the studies of prodrugs **28** in PBS. Interestingly, Tri*PPP*ro-NTPs **38** were also hydrolyzed to form γ-(AB)-NTPs as **43**

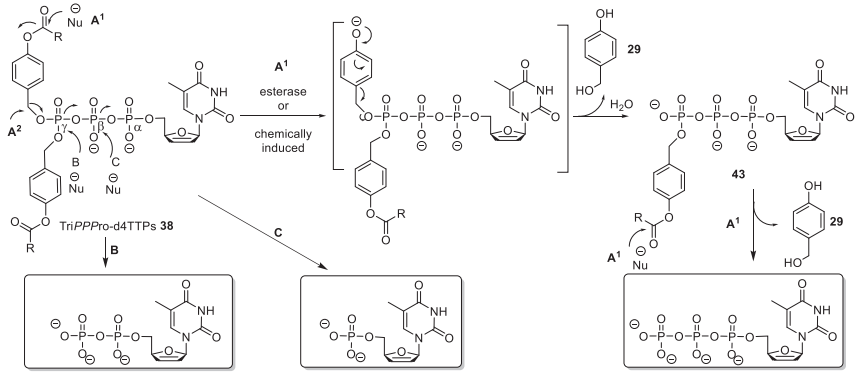

Scheme 14 Hydrolysis mechanism of Tri*PPP*ro-prodrugs **38** in PBS (pH 7.3) (shown for d4T as an example).

and then released the corresponding NTPs in PBS. The hydrolysis pathways leading to the different phosphorylated nucleotide metabolites are shown in Scheme 14.

The Tri*PPP*ro-concept is designed to be cleaved by esterases/lipases. As compared to the chemical hydrolyses, Tri*PPP*ro-compounds **38** were rapidly hydrolyzed with PLE and formed intermediates **43** demonstrating the enzymatic cleavage. The cleavage of intermediates **43** was again much slower than for Tri*PPP*ro-prodrugs **38**. Again, Tri*PPP*ro-compounds **38** were also readily cleaved to form intermediates **43** in CEM/0 cell extracts and then delivered the corresponding NTPs. In addition to NTPs (e.g., d4TTP, $t_{1/2} = 38$ min)[122] also a high amount of NDPs (e.g., d4TDP, $t_{1/2} = 59$ h)[122] were detected as well, probably due to the presence of dephosphorylating enzymes in cell extracts.

To confirm the Tri*PPP*ro-concept, primer extension assays were performed with HIV's reverse transcriptase (HIV-RT) after hydrolysis of γ-(AB-C8;AB-C8)-d4TTP. As expected, an immediate DNA chain termination was observed after incorporation of d4TMP, indicating that d4TTP (substrate for RT) was released from γ-(AB-C8;AB-C8)-d4TTP with PLE. Additionally, the thymidine-bearing γ-(AB-C8;AB-C8)-TTP was investigated in the same way. The hydrolysis of γ-(AB-C8;AB-C8)-TTP was performed and then the hydrolysis mixture was added to the polymerase assay. Here, the expected canonical incorporation of TMP was observed because the delivered TTP was accepted by HIV-RT as a substrate.

Tri*PPP*ro-prodrugs **38** were tested against HIV replication in infected wild-type (CEM/0) and TK-deficient (CEM/TK$^-$) cell cultures.

Tri*PPP*ro-d4TTPs **38** showed virtually similar activities against HIV-1 and HIV-2 as compared to the parent d4T in infected wild-type (CEM/0) cells. Importantly, good to very good antiviral activity of Tri*PPP*ro-d4TTPs **38** ($R \geq C_8H_{17}$) was detected in CEM/TK$^-$ cells with 15–535-fold improved activity as compared to the nucleoside. It was concluded from these studies that Tri*PPP*ro-d4TTPs **38** with biodegradable masking groups efficiently enter cells and deliver d4TTP, thereby bypass all intracellular phosphorylation steps. Again, Tri*PPP*ro-NTPs **38** (AB:C8;AB:C8) bearing different nucleoside analogs were active against HIV-1 and HIV-2 in infected wild-type (CEM/0) cell cultures, more importantly, they remained active in CEM/TK$^-$ cells as well.[123]

6.2 Non-symmetric Tri*PPP*ro-nucleoside triphosphate prodrugs

The first generation Tri*PPP*ro-prodrugs **38** comprised two *identical* biodegradable masking moieties and enabled the delivery of NTPs inside cells. In the case of Tri*PPP*ro-d4TTPs **38**, the desired cleavage of the phenol ester dominated, consequently, the prodrug mainly yielded the corresponding intermediates **43** and then released d4TTP (Scheme 14). From the results summarized for Tri*PPP*ro-d4TTPs **38**, the stability and antiviral activity were related to the alkyl chain length attached to the acyl residues. The shorter alkyl chain length led to lower stability of Tri*PPP*ro-d4TTPs **38** (AB:C1-C6) with no antiviral activity. In addition, Tri*PPP*ro-d4TTPs **38** (AB:C8-C15) comprising longer alkyl residues in the ester moiety exhibited higher chemical and biological stability and also higher antiviral activity. Compared to acyloxy ester Tri*PPP*ro-compounds, the alkyl carbonate functional groups (ACB) increase the stability of these prodrugs. These observations formed the basis for our research to conduct a study on a series of NTP prodrugs bearing two *different* biodegradable masking groups ($R^1 \neq R^2$). Non-symmetric Tri*PPP*ro-prodrugs bearing two *different* biodegradable masking groups (AB or ACB) are shown in Scheme 15.[126–128]

In 2020, we first described the non-symmetric γ-(AB;ACB)-d4TTPs (Scheme 15) with the aim to deliver d4TTP with high selectivity in PBS and by enzyme-triggered reactions in CEM cell extracts.[126] Studies have shown that the introduction of these different groups led to the selective formation of γ-(ACB)-d4TTPs **51** by chemical hydrolysis and in particular in cell extracts. Subsequently, the use of the Tri*PPP*ro-concept on a series of approved and also on so-far non-active nucleoside analogs was described to demonstrate the general applicability and the great potential that this approach

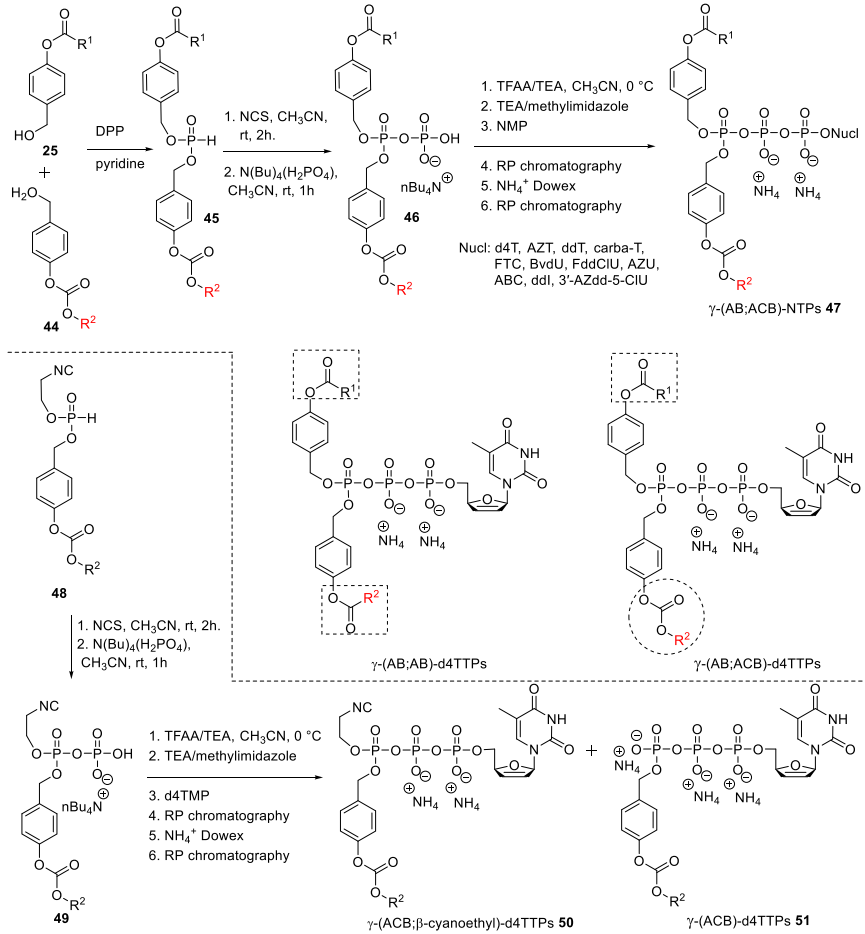

Scheme 15 Synthesis of Tri*PPP*ro-prodrugs **47** (d4T as an example) and intermediates **51** via *H*-phosphonate route.

promises (γ-(AB;ACB)-NTPs **47**; Scheme 15).[127] For comparison, we also made and studied Tri*PPP*ro-prodrugs (γ-(AB;AB)-d4TTPs) comprising two different AB moieties.[128]

6.3 Synthesis of non-symmetric Tri*PPP*ro-prodrugs 47 and γ-(ACB)-d4TTPs 51

Tri*PPP*ro-prodrugs **47** were preferably prepared using the *H*-phosphonate chemistry (up to 85% yield).[126–128] As shown in Scheme 15, the non-symmetric *H*-phosphonates **45** were stepwise activated with trifluoroacetic

acid anhydride (TFAA) and *N*-methylimidazole and reacted with d4TMP to yield Tri*PPP*ro-prodrugs **47**.[123] In addition to the γ-(AB;ACB)-d4TTPs **47**, the mono-masked intermediates **51** were synthesized as well (Scheme 15).[126] *H*-Phosphonates **48** were synthesized from DPP, 3-hydroxypropionitrile, and 4-alkoxycarbonyloxybenzyl alcohols **44**. *H*-Phosphonates **48** were converted into pyrophosphates **49** and then reacted with d4TMP to form γ-(ACB;β-cyanoethyl)-d4TTPs **50** (n-Bu_4N^+ form). It was found that the crude product was hydrolyzed during the ion-exchange to yield the mixture of γ-(ACB;β-cyanoethyl)-d4TTPs **50** (NH_4^+ form, yields of 52–63%) and γ-(ACB)-d4TTPs **51** (NH_4^+ form, yields of 10–23%). We assumed that the β-cyanoethyl protecting group was cleaved by the known β-elimination leading to γ-(ACB)-d4TTPs **51**.

As before, Tri*PPP*ro-prodrugs **47** were studied in PBS (25 mM, pH 7.3), pig liver esterase (PLE), and CEM cell extracts. The calculated half-lives of prodrugs **47** reflect the removal of the AB group and/or the ACB group to yield the corresponding intermediates, γ-(AB)-d4TTPs **43** and γ-(ACB)-d4TTPs **51**, respectively. Possible hydrolysis pathways of Tri*PPP*ro-d4TTPs **47** are summarized in Scheme 16.

Generally, the chemical stability of Tri*PPP*ro-d4TTPs **47** (AB-C2;ACB: C9-C16) ($t_{1/2}$ = 25–83 h) increased with increasing alkyl chain lengths. However, half-lives of more lipophilic compounds **47** (AB-C3-C9;ACB: C12-C18) remained in the same range ($t_{1/2}$ = 74–90 h).[126] The half-lives of the carbonate intermediates **51** were significantly higher than those of

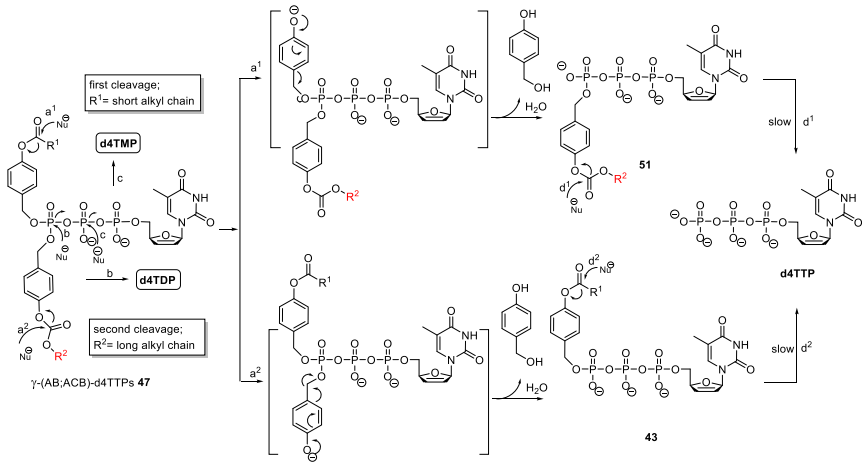

Scheme 16 Hydrolysis and delivery mechanism of Tri*PPP*ro-d4TTPs **47**.

γ-(AB;ACB)-d4TTPs **47**. Moreover, chemical stabilities of γ-alkyl carbonate bearing γ-(ACB)-d4TTPs **51** were higher than the corresponding ester intermediates γ-(AB)-d4TTPs **43**, which was in full agreement with the results observed from the studies of γ-(AB;ACB)-d4TTPs **47** in PBS. The half-life for γ-(ACB-C16)-d4TTP ($t_{1/2} > 1600$ h)[126] was almost 3-fold higher as compared to the studies of γ-(AB-C17)-d4TTP ($t_{1/2} =$ 580 h)[122] described before. In the case of γ-(AB-C11;ACB-C6)-d4TTP, the γ-(AB-C11)-d4TTP/γ-(ACB-C6)-d4TTP ratio was found to be 1:3. In addition, the half-life of γ-(AB-C11)-d4TTP ($t_{1/2} = 460$ h)[122] was also found to be lower than that for γ-(ACB-C6)-d4TTP ($t_{1/2} = 540$ h).[126]

As an example, when γ-(AB-C2;ACB-C16)-d4TTP[126] was totally consumed after incubation for 50 days in PBS, both intermediates γ-(ACB-C16)-d4TTP (mainly) and γ-(AB-C2)-d4TTP (trace) were formed although in very different concentration and thus, the hydrolysis proceeded highly selective. Both masking groups of γ-(AB;ACB)-d4TTPs **47** were involved in the chemical hydrolysis pathway a^1 and pathway a^2 (Scheme 16). Before complete consumption of the starting γ-(AB-C2;ACB-C16)-d4TTP, an increase of d4TTP and γ-(ACB-C16)-d4TTP concentrations and a very small amount of γ-(AB-C2)-d4TTP were observed, which supports that the γ-(AB-C2)-d4TTP was prone to hydrolysis to form d4TTP.

With PLE, Tri*PPP*ro-compounds **47** were rapidly hydrolyzed ($t_{1/2} = 0.17$–13.8 h).[126–128] In the case of the enzymatically catalyzed hydrolysis of γ-(AB-C4;ACB-C16)-NTPs **47**, both hydrolysis intermediates γ-(ACB-C16)-NTPs and γ-(AB-C4)-NTPs were formed in markedly different amounts. Both intermediates first accumulated and later were slowly hydrolyzed to yield NTPs. As in PBS, the highly selective cleavage of the AB group (e.g., AB-C2) led to the formation of γ-(ACB-C16)-NTPs. In contrast, for the hydrolysis of γ-(AB-C4;AB-C15)-d4TTP, both possible intermediates γ-(AB-C14)-d4TTP and γ-(AB-C15)-d4TTP were formed in almost identical amounts.

As before, Tri*PPP*ro-compounds **47** were quickly hydrolyzed in CEM/0 cell extracts and delivered the two intermediates. However, the stabilities of γ-(AB;ACB)-d4TTPs were in the range of 0.8–6.4 h without showing a clear trend. Interestingly, our studies have shown that γ-(AB;ACB)-d4TTPs were readily cleaved to form intermediates γ-(ACB)-d4TTPs **51** but in low concentrations in CEM/0 cell extracts. In addition, a small amount of d4TTP and a large amount of d4TDP were detected due to the fast dephosphorylation of the d4TTP ($t_{1/2} = 38$ min)[122] by

phosphorylases/kinases present in the cell extracts. These results were in line with the previous results of the symmetric Tri*PPP*ro-prodrugs **38**. Moreover, in case of γ-(AB-C11;ACB-C6)-d4TTP, a predominant formation of γ-(ACB-C6)-d4TTP was observed, the ratio of γ-(AB-C11)-d4TTP and γ-(ACB-C6)-d4TTP was 1:10 after 8 h incubation in CEM/0 cell extracts. This was in full agreement with the results obtained from the studies of this compound in PBS that an almost selective cleavage took place in cell extracts with the AB-moiety being cleaved first. More importantly, it was proven that NTPs were also successfully released from the Tri*PPP*ro-NTPs **47** (AB-C4;ACB:C16) in cell extracts.[127] In all cases, the enzymatic cleavage also took place for the mono-masked intermediates γ-(AB-C4)-NTPs and γ-(ACB-C6)-NTPs, respectively. Again, NTPs were detected in low concentrations only because of the fast enzymatic dephosphorylation by phosphorylases/kinases (main product) and ultimately NMPs. In contrast to γ-(AB-C2; ACB-C16)-d4TTP, no selective cleavage of the different AB-masks of γ-(AB;AB)-d4TTPs was observed in the hydrolysis in CEM cell extracts.[128]

Prodrugs **47** and intermediates **51** were evaluated for HIV replication inhibition in HIV-1/2-infected wild-type CEM/0 cells and in HIV-2-infected mutant thymidine kinase-deficient (CEM/TK$^-$) cells, and the different nucleoside analogs as reference compounds. For γ-(AB-C2; ACB-C16)-d4TTP ($EC_{50}=0.027$ μM/HIV-1, $EC_{50}=0.0048$ μM/HIV-2), the antiviral activity in this infected cell line improved by 16-fold and 65-fold, respectively, as compared to d4T ($EC_{50}=0.43$ μM/HIV-1, $EC_{50}=0.31$ μM/HIV-2).[126] More importantly, also high activities were obtained depending on the lipophilicity of the γ-(AB;ACB)-d4TTPs against HIV-2 in this thymidine kinase-deficient (CEM/TK$^-$) cell model. With γ-(AB-C2;ACB-C16)-d4TTP ($EC_{50}=0.11$ μM/HIV-2) the antiviral activity in this infected cell line was improved by a 282-fold as compared to d4T ($EC_{50}=31.05$ μM/HIV-2). However, the antiviral activity detected in CEM/0 cell cultures decreased in the case of γ-(AB-C2;ACB-C16)-d4TTP in CEM/TK$^-$ cells (23-fold), potentially due to the instability of the these prodrugs in addition to a fast cleavage of the bioreversible AB- or ACB-moiety. We speculated that γ-(AB;ACB)-d4TTPs **47** were rapidly hydrolyzed in cell extracts and d4TTP was present in insufficient concentrations (fast dephosphorylation) to exhibit anti-HIV activity in cells. Moreover, it cannot be excluded that the antiviral activity observed in the infected CEM/TK$^-$ deficient cells was at least in part due to the formation of d4TDP and d4TMP. In the hydrolysis of γ-(AB-C2;ACB-C16)-d4TTP in cell extracts, a large amount of d4TDP and some d4TMP were detected.[126]

Interestingly, the intermediate γ-(ACB-C16)-d4TTP ($EC_{50} = 1.46$ μM/HIV-2) was also potent in CEM/TK$^-$ cell cultures, indicating that even *one* long aliphatic chain in the ACB-units provides enough lipophilicity to enable a cellular uptake of the aliphatic γ-(AB;ACB)-d4TTPs.

More interestingly, the high potential of the Tri*PPP*ro-approach was also demonstrated by the nucleoside triphosphate prodrugs **47** bearing different nucleoside analogs.[127] These prodrugs proved also highly potent in CEM/TK$^-$ cells, whereas their parent nucleosides lacked any relevant antiviral activity in wild-type CEM/0 cell model. It was confirmed that these Tri*PPP*ro-NTPs **47** were also taken-up by the cells and delivered intracellularly a phosphorylated form of the parent nucleosides, most likely NTPs. Therefore, it was confirmed that the Tri*PPP*ro-strategy enabled the intracellular delivery of NTPs, and the concept could be used to convert inactive nucleoside analogs into powerful biologically active metabolites.

6.4 Nucleoside triphosphate prodrugs: T-1106-Tri*PPP*ro-prodrugs

Encouraged by the previously obtained results, we synthesized two T-1106-Tri*PPP*ro prodrugs **52**, the symmetrical T-1106-Tri*PPP*ro prodrug **52a** (AB-C9;AB-C9) and the non-symmetrical T-1106-Tri*PPP*ro prodrug **52b** (AB-C4;AB-C14), with the aim of achieving metabolic bypass and superior antiviral potency.[46] T-1106-Tri*PPP*ro-prodrugs **52** were prepared using the phosphoramidite protocol (Scheme 17).[110,113] The conversion of T-1106-RDP to T-1106-Tri*PPP*ro prodrugs **52a**,**b** resulted in yields of 27% and 44%. Due to the already mentioned stability problems, until now we were unable to synthesize the T-705-RTP prodrug. T-1106-Tri*PPP*ro prodrugs **52** were also studied with regard to their chemical and biological stabilities and their hydrolysis products in PBS (pH 7.3, Fig. 4B, condition without esterase), PLE (Fig. 4B, condition with esterase), and crude enzyme preparations (i.e., MDCK and MDCK TG^{res} cell extracts) (Fig. 5). Additionally, these prodrugs were evaluated for their anti-influenza virus activity in wild-type and HGPRT-deficient cells.

Similar to the cleavage pathway for Tri*PPP*ro-d4TTPs **38**, T-1106-Tri*PPP*ro prodrug **52a** (AB-C9;AB-C9) was hydrolyzed to give the mono-masked intermediate **53** (AB-C9) with some concomitant cleavage to T-1105-RTP and subsequently T-1105-RDP (Fig. 4B). Interestingly, the mono-masked triphosphate intermediates **53** proved to be more stable than the corresponding mono-masked T-1106-Di*PP*ro-compounds **37** (Fig. 4A and B). However, when T-1106-Tri*PPP*ro-prodrugs **52a**,**b** were exposed

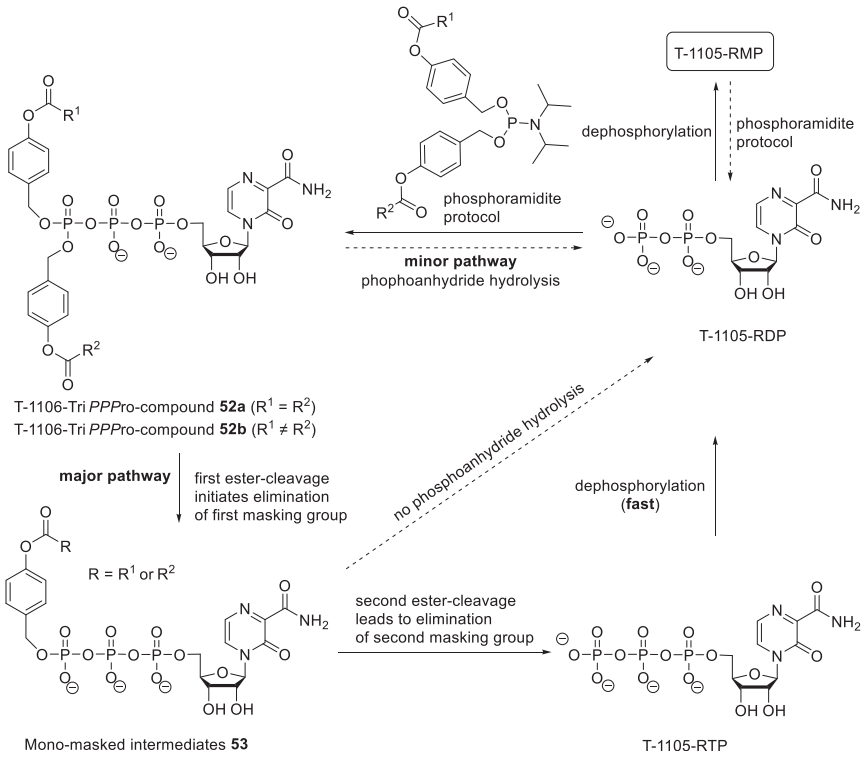

Scheme 17 Synthesis and hydrolysis mechanism of T-1106-Tri*PPP*ro-prodrugs **52**.

to crude enzyme preparations (i.e., MDCK or MDCK TG^{res} cell extracts), no T-1105-RTP was observed, probably due to its fast dephosphorylation after initial formation (Fig. 5). Compared to the T-1106-Di*PP*ro-prodrugs **36**, after 2 h incubation, a higher amount of T-1105-RDP was detected from the corresponding T-1106-Tri*PPP*ro-prodrugs **52a**,**b** (Fig. 5, compare dark gray stacks). As shown in Fig. 5, the stability of the T-1106-Tri*PPP*ro-prodrugs **52a**,**b** was found to be lower than the corresponding T-1106-Di*PP*ro-prodrugs **36a**,**b**, respectively. In addition, the enzymatic cleavage of the symmetric T-1106-Tri*PPP*ro-prodrug **52a** proceeded faster than the non-symmetric T-1106-Tri*PPP*ro-prodrug **52b**.

The anti-influenza activity of T-1106-Tri*PPP*ro-prodrugs **52a**,**b** in MDCK and MDCK-TG^{res} cells was lower as compared to T-1106-Di*PP*ro-prodrugs **36a**,**b** (Table 1). T-1106-Tri*PPP*ro-prodrugs **52a** (AB-C9;AB-C9) and **52b** (AB-C4;AB-C14) had EC_{50} values of 2.8 μM and 7.2 μM, respectively. We assumed that the difference in antiviral activity

may be caused by the differences in cell membrane permeability. Moreover, this ranking in antiviral activity corresponds to the ranking in activation rate (Fig. 5). Interestingly, T-1106-Tri*PPP*ro prodrugs **52a**,**b** also retained their anti-influenza activity in HGPRT-deficient MDCK-TG^{res} cells. For instance, T-1106-Tri*PPP*ro-prodrugs **52a** (AB-C9;AB-C9) had an average EC_{50} value of 2.8 μM in MDCK cells versus 2.5 μM in MDCK-TG^{res} cells (Table 1). Therefore, the T-1106-Tri*PPP*ro-prodrugs **52** were successfully released T-1105-RTP, thus bypassing their HGPRT and kinase dependence (Fig. 1). The T-1106-Tri*PPP*ro-prodrugs **52** enabled the bypass the second step of the intracellular phosphorylation in cells, i.e., phosphorylation of T-1105-RMP to T-1105-RDP. We proved that the conversion of T-1106-RDP into T-1106-RTP was not limiting. This was shown in enzymatic studies.

7. Conclusion

The results summarized in this minireview show that nucleoside analogs still have enormous potential to be used as antivirals mainly as inhibitors of the viral polymerases as described here with the example of T-1105-RTP and the RNA-dependent-RNA-polymerase of SARS-CoV-2. Although this polymerase has a proof-reading system, the incorporated T-1105-RMP at least in part escapes its repair after incorporation. With the already known broad-spectrum antiviral activity of Favipiravir (T-705) this may also lead in the case of T-1105 or even other derivatives thereof to broad spectrum antivirals. Moreover, the application of nucleotide delivery approaches may contribute significantly to the improvement of antivirally active nucleoside analogs. This was already accepted in the past for the use of nucleoside monophosphate prodrugs such as the phosphoramidate system, but here we described results that in other cases the intracellular delivery of nucleoside monophosphates is not sufficient for the improvement of the antiviral activity due to metabolic hurdles that appear after the conversion into the monophosphate. In such cases nucleoside di- or even nucleoside triphosphate prodrug systems can help to overcome these limitations. This has been shown here by the failure of the application of the *cyclo*Sal-nucleoside monophosphate delivery approach and the use of the Di*PP*ro- or the Tri*PPP*ro-nucleoside di- or triphosphate compounds. The chemical synthesis routes towards these latter compounds are now robust and can be applied to a large variety of nucleoside analogs. We are convinced that the further development of these prodrug systems of higher phosphorylated nucleosides will have an important impact in nucleoside drug development.

References

1. *Annual Review of Diseases Prioritized Under the Research and Development Blueprint*; WHO Research and Development Blueprint, 2018.
2. Iuliano, A. D.; Roguski, K. M.; Chang, H. H. Estimates of Global Seasonal Influenza-Associated Respiratory Mortality: A Modelling Study. *Lancet* **2018**, *391*, 1285–1300.
3. Kaner, J.; Schaack, S. Understanding Ebola: The 2014 Epidemic. Glob. Health 2016, 12, 53–60.
4. Xia, H. J.; Xie, X. P.; Shan, C.; Shi, P. Y. Potential Mechanisms for Enhanced Zika Epidemic and Disease. *Acs Infect. Dis.* **2018**, *4*, 656–659.
5. Wu, F.; Zhao, S.; Yu, B.; Chen, Y. M.; Wang, W.; Song, Z. G.; Hu, Y.; Tao, Z. W.; Tian, J. H.; Pei, Y. Y.; Yuan, M. L.; Zhang, Y. L.; Dai, F. H.; Liu, Y.; Wang, Q. M.; Zheng, J. J.; Xu, L.; Holmes, E. C.; Zhang, Y. Z. A New Coronavirus Associated with Human Respiratory Disease in China. *Nature* **2020**, *579*, 265–269.
6. Zhu, N.; Zhang, D. Y.; Wang, W. L.; Li, X. W.; Yang, B.; Song, J. D.; Zhao, X.; Huang, B. Y.; Shi, W. F.; Lu, R. J.; Niu, P. H.; Zhan, F. X.; Ma, X. J.; Wang, D. Y.; Xu, W. B.; Wu, G. Z.; Gao, G. G. F.; Tan, W. J.; Coronavirus, C. N. A Novel Coronavirus from Patients with Pneumonia in China, 2019. *N. Engl. J. Med.* **2020**, *382*, 727–733.
7. WHO. Coronavirus (COVID-19) Dashboard, 2021. https://www.who.int/emergencies/diseases/novel-coronavirus-2019 (accessed September 9, 2021).
8. Wu, R.; Wang, L.; Kuo, H. D.; Shannar, A.; Peter, R.; Chou, P. J.; Li, S.; Hudlikar, R.; Liu, X.; Liu, Z.; Poiani, G. J.; Amorosa, L.; Brunetti, L.; Kong, A. N. An Update on Current Therapeutic Drugs Treating COVID-19. *Curr. Pharmacol. Rep.* **2020**, 1–15.
9. Chaudhuri, S.; Symons, J. A.; Deval, J. Innovation and Trends in the Development and Approval of Antiviral Medicines: 1987-2017 and Beyond. *Antivir. Res.* **2018**, *155*, 76–88.
10. Burton, J. R.; Everson, G. T. HCV NS5B Polymerase Inhibitors. *Clin. Liver Dis.* **2009**, *13*, 453–465.
11. Cihlar, T.; Ray, A. S. Nucleoside and Nucleotide HIV Reverse Transcriptase Inhibitors: 25 Years after Zidovudine. *Antivir. Res.* **2010**, *85*, 39–58.
12. Jordheim, L. P.; Durantel, D.; Zoulim, F.; Dumontet, C. Advances in the Development of Nucleoside and Nucleotide Analogues for cancer and Viral Diseases. *Nat. Rev. Drug Discov.* **2013**, *12*, 447–464.
13. Deval, J. Antimicrobial Strategies Inhibition of Viral Polymerases by 3′-Hydroxyl Nucleosides. *Drugs* **2009**, *69*, 151–166.
14. Wang, G. Y.; Wan, J. G.; Hu, Y. J.; Wu, X. Y.; Prhavc, M.; Dyatkina, N.; Rajwanshi, V. K.; Smith, D. B.; Jekle, A.; Kinkade, A.; Symons, J. A.; Jin, Z. N.; Deval, J.; Zhang, Q. L.; Tam, Y.; Chanda, S.; Blatt, L.; Beigelman, L. Synthesis and Anti-Influenza Activity of Pyridine, Pyridazine, and Pyrimidine C-Nucleosides as Favipiravir (T-705) Analogues. *J. Med. Chem.* **2016**, *59*, 4611–4624.
15. Atta, M. G.; De Seigneux, S.; Lucas, G. M. Clinical Pharmacology in HIV Therapy. *Clin. J. Am. Soc. Nephrol.* **2019**, *14*, 435–444.
16. Li, G. D.; De Clercq, E. Therapeutic Options for the 2019 Novel Coronavirus (2019-nCoV). *Nat. Rev. Drug Discov.* **2020**, *19*, 149–150.
17. Elfiky, A.; Ribavirin, A. Remdesivir, Sofosbuvir, Galidesivir, and Tenofovir Against SARS-CoV-2 RNA Dependent RNA Polymerase (RdRp): A Molecular Docking Study. *Life Sci.* **2020**, *253*, 117592.
18. Furuta, Y.; Gowen, B. B.; Takahashi, K.; Shiraki, K.; Smee, D. F.; Barnard, D. L. Favipiravir (T-705), a Novel Viral RNA Polymerase Inhibitor. *Antivir. Res.* **2013**, *100*, 446–454.

19. Furuta, Y.; Takahashi, K.; Shiraki, K.; Sakamoto, K.; Smee, D. F.; Barnard, D. L.; Gowen, B. B.; Julander, J. G.; Morrey, J. D. T-705 (Favipiravir) and Related Compounds: Novel Broad-Spectrum Inhibitors of RNA Viral Infections. *Antivir. Res.* **2009**, *82*, 95–102.
20. Takahashi, K.; Furuta, Y.; Fukuda, Y.; Kuno, M.; Kamiyama, T.; Kozaki, K.; Nomura, N.; Egawa, H.; Minami, S.; Shiraki, K. In Vitro and In Vivo Activities of T-705 and Oseltamivir against Influenza Virus. *Antivir. Chem. Chemother.* **2003**, *14*, 235–241.
21. Furuta, Y.; Takahashi, K.; Fukuda, Y.; Kuno, M.; Kamiyama, T.; Kozaki, K.; Nomura, N.; Egawa, H.; Minami, S.; Watanabe, Y.; Narita, H.; Shiraki, K. In Vitro and In Vivo Activities of Anti-Influenza Virus Compound T-705. *Antimicrob. Agents Chemother.* **2002**, *46*, 977–981.
22. Furuta, Y.; Takahashi, K.; Kuno-Maekawa, M.; Sangawa, H.; Uehara, S.; Kozaki, K.; Nomura, N.; Egawa, H.; Shiraki, K. Mechanism of Action of T-705 Against Influenza Virus. *Antimicrob. Agents Chemother.* **2005**, *49*, 981–986.
23. Oestereich, L.; Rieger, T.; Ludtke, A.; Ruibal, P.; Wurr, S.; Pallasch, E.; Bockholt, S.; Krasemann, S.; Munoz-Fontela, C.; Gunther, S. Efficacy of Favipiravir Alone and in Combination with Ribavirin in a Lethal, Immunocompetent Mouse Model of Lassa Fever. *J. Infect. Dis.* **2016**, *213*, 934–938.
24. Tani, H.; Fukuma, A.; Fukushi, S.; et al. Efficacy of T-705 (Favipiravir) in the Treatment of Infections with Lethal Severe Fever with Thrombocytopenia Syndrome Virus. *mSphere* **2016**, *1*, e00061–15.
25. Oestereich, L.; Ludtke, A.; Wurr, S.; Rieger, T.; Munoz-Fontela, C.; Gunther, S. Successful Treatment of Advanced Ebola Virus Infection with T-705 (Favipiravir) in a Small Animal Model. *Antivir. Res.* **2014**, *105*, 17–21.
26. Yamada, K.; Noguchi, K.; Komeno, T.; Furuta, Y.; Nishizono, A. Efficacy of Favipiravir (T-705) in Rabies Postexposure Prophylaxis. *J. Infect. Dis.* **2016**, *213*, 1253–1261.
27. Delang, L.; Guerrero, N. S.; Tas, A.; Querat, G.; Pastorino, B.; Froeyen, M.; Dallmeier, K.; Jochmans, D.; Herdewijn, P.; Bello, F.; Snijder, E. J.; de Lamballerie, X.; Martina, B.; Neyts, J.; van Hemert, M. J.; Leyssen, P. Mutations in the Chikungunya Virus Non-structural Proteins Cause Resistance to Favipiravir (T-705), a Broad-Spectrum Antiviral. *J. Antimicrob. Chemother.* **2014**, *69*, 2770–2784.
28. Julander, J. G.; Smee, D. F.; Morrey, J. D.; Furuta, Y. Effect of T-705 Treatment on Western Equine Encephalitis in a Mouse Model. *Antivir. Res.* **2009**, *82*, 169–171.
29. Morrey, J. D.; Taro, B. S.; Siddharthan, V.; Wang, H.; Smee, D. F.; Christensen, A. J.; Furuta, Y. Efficacy of Orally Administered T-705 Pyrazine Analog on Lethal West Nile Virus Infection in Rodents. *Antivir. Res.* **2008**, *80*, 377–379.
30. Scharton, D.; Bailey, K. W.; Vest, Z.; Westover, J. B.; Kumaki, Y.; Van Wettere, A.; Furuta, Y.; Gowen, B. B. Favipiravir (T-705) Protects against Peracute Rift Valley Fever Virus Infection and Reduces Delayed-Onset Neurologic Disease Observed with Ribavirin Treatment. *Antivir. Res.* **2014**, *104*, 84–92.
31. Oestereich, L.; Rieger, T.; Neumann, M.; Bernreuther, C.; Lehmann, M.; Krasemann, S.; Wurr, S.; Emmerich, P.; de Lamballerie, X.; Olschlager, S.; Gunther, S. Evaluation of Antiviral Efficacy of Ribavirin, Arbidol, and T-705 (Favipiravir) in a Mouse Model for Crimean-Congo Hemorrhagic Fever. *PLoS Negl. Trop. Dis.* **2014**, *8*, e2804.
32. Julander, J. G.; Shafer, K.; Smee, D. F.; Morrey, J. D.; Furuta, Y. Activity of T-705 in a hamster Model of Yellow Fever Virus Infection in Comparison with that of a Chemically Related Compound, T-1106. *Antimicrob. Agents Chemother.* **2009**, *53*, 202–209.
33. Safronetz, D.; Falzarano, D.; Scott, D. P.; Furuta, Y.; Feldmann, H.; Gowen, B. B. Antiviral Efficacy of Favipiravir against Two Prominent Etiological Agents of Hantavirus Pulmonary Syndrome. *Antimicrob. Agents Chemother.* **2013**, *57*, 4673–4680.

34. De Clercq, E.; Li, G. D. Approved Antiviral Drugs over the Past 50 Years. *Clin. Microbiol. Rev.* **2016**, *29*, 695–747.
35. Cai, Q. X.; Yang, M. H.; Liu, D. J.; Chen, J.; Shu, D.; Xia, J. X.; Liao, X. J.; Gu, Y. B.; Cai, Q.; Yang, Y.; Shen, C. G.; Li, X. H.; Peng, L.; Huang, D. L.; Zhang, J.; Zhang, S. R.; Wang, F. X.; Liu, J. Y.; Chen, L.; Chen, S. Y.; Wang, Z. Q.; Zhang, Z.; Cao, R. Y.; Zhong, W.; Liu, Y. X.; Liu, L. Experimental Treatment with Favipiravir for COVID-19: An Open-Label Control Study. *Engineering* **2020**, *6*, 1192–1198.
36. Yamamura, H.; Matsuura, H.; Nakagawa, J.; et al. Effect of Favipiravir and an Anti-Inflammatory Strategy for COVID-19. *Crit. Care* **2020**, *24*, 413.
37. Chen, C.; Zhang, Y.; Huang, J.; Yin, P.; Cheng, Z.; Wu, J.; Chen, S.; Zhang, Y.; Chen, B.; Lu, M.; Luo, Y.; Ju, L.; Zhang, J.; Wang, X. Favipiravir Versus Arbidol for COVID-19: A Randomized Clinical Trial. *medRxiv* **2020**, https://doi.org/10.1101/2020.03.17.20037432.
38. Smee, D. F.; Hurst, B. L.; Egawa, H.; Takahashi, K.; Kadota, T.; Furuta, Y. Intracellular Metabolism of Favipiravir (T-705) in Uninfected and Influenza A (H5N1) Virus-Infected Cells. *J. Antimicrob. Chemother.* **2009**, *64*, 741–746.
39. Naesens, L.; Guddat, L. W.; Keough, D. T.; van Kuilenburg, A. B. P.; Meijer, J.; Vande Voorde, J.; Balzarini, J. Role of Human Hypoxanthine Guanine Phosphoribosyltransferase in Activation of the Antiviral Agent T-705 (Favipiravir). *Mol. Pharmacol.* **2013**, *84*, 615–629.
40. Yu, X. J.; Liang, M. F.; Zhang, S. Y.; Liu, Y.; Li, J. D.; Sun, Y. L.; Zhang, L. H.; Zhang, Q. F.; Popov, V. L.; Li, C.; Qu, J.; Li, Q.; Zhang, Y. P.; Hai, R.; Wu, W.; Wang, Q.; Zhan, F. X.; Wang, X. J.; Kan, B.; Wang, S. W.; Wan, K. L.; Jing, H. Q.; Lu, J. X.; Yin, W. W.; Zhou, H.; Guan, X. H.; Liu, J. F.; Bi, Z. Q.; Liu, G. H.; Ren, J.; Wang, H.; Zhao, Z.; Song, J. D.; He, J. R.; Wan, T.; Zhang, J. S.; Fu, X. P.; Sun, L. N.; Dong, X. P.; Feng, Z. J.; Yang, W. Z.; Hong, T.; Zhang, Y.; Walker, D. H.; Wang, Y.; Li, D. X. Fever with Thrombocytopenia Associated with a Novel Bunyavirus in China. *N Engl J Med* **2011**, *364*, 1523–1532.
41. Kaptein, S. J. F.; Jacobs, S.; Langendries, L.; Seldeslachts, L.; ter Horst, S.; Liesenborghs, L.; Hens, B.; Vergote, V.; Heylen, E.; Barthelemy, K.; Maas, E.; De Keyzer, C.; Bervoets, L.; Rymenants, J.; Van Buyten, T.; Zhang, X.; Abdelnabi, R.; Pang, J.; Williams, R.; Thibaut, H. J.; Dallmeier, K.; Boudewijns, R.; Wouters, J.; Augustijns, P.; Verougstraete, N.; Cawthorne, C.; Breuer, J.; Solas, C.; Weynand, B.; Annaert, P.; Spriet, I.; Velde, G. V.; Neyts, J.; Rocha-Pereira, J.; Delang, L. Favipiravir at High Doses Has Potent Antiviral Activity in SARS-CoV-2-Infected Hamsters, Whereas Hydroxychloroquine Lacks Activity. *Proc Natl Acad Sci USA* **2020**, *117*, 26955–26965.
42. Nagata, T.; Lefor, A. K.; Hasegawa, M.; Ishii, M. Favipiravir: A New Medication for the Ebola Virus Disease Pandemic. *Disaster Med. Public Health Prep.* **2015**, *9*, 79–81.
43. Huchting, J.; Vanderlinden, E.; Van Berwaer, R.; Meier, C.; Naesens, L. Cell Line-Dependent Activation and Antiviral Activity of T-1105, the Non-fluorinated Analogue of T-705 (Favipiravir). *Antivir. Res.* **2019**, *167*, 1–5.
44. Gowen, B. B.; Wong, M. H.; Jung, K. H.; Sanders, A. B.; Mendenhall, M.; Bailey, K. W.; Furuta, Y.; Sidwell, R. W. In Vitro and In Vivo Activities of T-705 against Arenavirus and Bunyavirus Infections. *Antimicrob. Agents Chemother.* **2007**, *51*, 3168–3176.
45. Sidwell, R. W.; Barnard, D. L.; Day, C. W.; Smee, D. F.; Bailey, K. W.; Wong, M. H.; Morrey, J. D.; Furuta, Y. Efficacy of Orally Administered T-705 on Lethal Avian Influenza a (H5N1) Virus Infections in Mice. *Antimicrob. Agents Chemother.* **2007**, *51*, 845–851.

46. Huchting, J.; Vanderlinden, E.; Winkler, M.; Nasser, H.; Naesens, L.; Meier, C. Prodrugs of the Phosphoribosylated Forms of Hydroxypyrazinecarboxamide Pseudobase T-705 and its de-Fluoro Analogue T-1105 as Potent Influenza Virus Inhibitors. *J. Med. Chem.* **2018**, *61*, 6193–6210.
47. Eriksson, B.; Helgstrand, E.; Johansson, N. G.; Larsson, A.; Misiorny, A.; Noren, J. O.; Philipson, L.; Stenberg, K.; Stening, G.; Stridh, S.; Oberg, B. Inhibition of Influenza-Virus Ribonucleic-Acid Polymerase by Ribavirin Triphosphate. *Antimicrob. Agents Chemother.* **1977**, *11*, 946–951.
48. Reguera, J.; Gerlach, P.; Cusack, S. Towards a Structural Understanding of RNA Synthesis by Negative Strand RNA Viral Polymerases. *Curr. Opin. Struct. Biol.* **2016**, *36*, 75–84.
49. Ortin, J.; Martin-Benito, J. The RNA Synthesis Machinery of Negative-Stranded RNA Viruses. *Virology* **2015**, *479*, 532–544.
50. Ogando, N. S.; Zevenhoven-Dobbe, J. C.; Meer, Y. V. D.; Bredenbeek, P. J.; Posthuma, C. C.; Snijder, E. J.; Gallagher, T. The Enzymatic Activity of the nsp14 Exoribonuclease Is Critical for Replication of MERS-CoV and SARS-CoV-2. *J. Virol.* **2020**, *94*, e01246–20.
51. Robson, F.; Khan, K. S.; Le, T. K.; Paris, C.; Demirbag, S.; Barfuss, P.; Rocchi, P.; Ng, W.-L. Coronavirus RNA Proofreading: Molecular Basis and Therapeutic Targeting. *Mol. Cell* **2020**, *79*, 710–727.
52. Ferron, F.; Subissi, L.; Silveira De Morais, A. T.; Le, N. T. T.; Sevajol, M.; Gluais, L.; Decroly, E.; Vonrhein, C.; Bricogne, G.; Canard, B.; Imbert, I. Structural and Molecular Basis of Mismatch Correction and Ribavirin Excision from Coronavirus RNA. *PNAS* **2018**, *115*, E162.
53. Sheahan, T. P.; Sims, A. C.; Zhou, S.; Graham, R. L.; Pruijssers, A. J.; Agostini, M. L.; Leist, S. R.; Schäfer, A.; Dinnon, K. H.; Stevens, L. J.; Chappell, J. D.; Lu, X.; Hughes, T. M.; George, A. S.; Hill, C. S.; Montgomery, S. A.; Brown, A. J.; Bluemling, G. R.; Natchus, M. G.; Saindane, M.; Kolykhalov, A. A.; Painter, G.; Harcourt, J.; Tamin, A.; Thornburg, N. J.; Swanstrom, R.; Denison, M. R.; Baric, R. S. An Orally Bioavailable Broad-Spectrum Antiviral Inhibits SARS-CoV-2 in Human Airway Epithelial Cell Cultures and Multiple Coronaviruses in Mice. *Sci. Transl. Med.* **2020**, *12*, eabb5883.
54. Lo, H. S.; Hui, K. P. Y.; Lai, H.-M.; Khan, K. S.; Kaur, S.; Huang, J.; Li, Z.; Chan, A. K. N.; Cheung, H. H.-Y.; Ng, K.-C.; Wang Ho, J. C.; Chen, Y. W.; Ma, B.; Cheung, P. M.-H.; Shin, D.; Wang, K.; Lee, M.-H.; Selisko, B.; Eydoux, C.; Guillemot, J.-C.; Canard, B.; Wu, K.-P.; Liang, P.-H.; Dikic, I.; Zuo, Z.; Chan, F. K. L.; Hui, D. S. C.; Mok, V. C. T.; Wong, K.-B.; Ko, H.; Aik, W. S.; Chan, M. C. W.; Ng, W.-L. Simeprevir Potently Suppresses SARS-CoV-2 Replication and Synergizes with Remdesivir. *ACS Cent. Sci.* **2021**, *7*, 792–802.
55. Goldhill, D. H.; Langat, P.; Xie, H.; Galiano, M.; Miah, S.; Kellam, P.; Zambon, M.; Lackenby, A.; Barclay, W. S. J. J. O. V. Determining the Mutation Bias of Favipiravir in Influenza Virus Using Next-Generation Sequencing. *J. Virol.* **2019**, *93*, e01217–18.
56. Baranovich, T.; Wong, S.-S.; Armstrong, J.; Marjuki, H.; Webby, R. J.; Webster, R. G.; Govorkova, E. A. J. J. O. V. T-705 (Favipiravir) Induces Lethal Mutagenesis in Influenza A H1N1 Viruses In Vitro. *J. Virol.* **2013**, *87*, 3741–3751.
57. Escribano-Romero, E.; Jimenez de Oya, N.; Domingo, E.; Saiz, J. C. J. A. A. Chemotherapy. Extinction of West Nile virus by Favipiravir Through Lethal Mutagenesis. *Antimicrob. Agents Chemother.* **2017**, *61*, e01400–17.
58. De Ávila, A. I.; Gallego, I.; Soria, M. E.; et al. Lethal Mutagenesis of Hepatitis C Virus Induced by Favipiravir. *Plos One* **2016**, *11*, e0164691.
59. Arias, A.; Thorne, L.; Goodfellow, I. J. E. Favipiravir Elicits Antiviral Mutagenesis During Virus Replication In Vivo. *eLife* **2014**, *3*, e03679.

60. Sangawa, H.; Komeno, T.; Nishikawa, H.; Yoshida, A.; Takahashi, K.; Nomura, N.; Furuta, Y. Mechanism of Action of T-705 Ribosyl Triphosphate against Influenza Virus RNA Polymerase. *Antimicrob. Agents Chemother.* **2013**, *57*, 5202–5208.
61. Jin, Z. N.; Smith, L. K.; Rajwanshi, V. K.; Kim, B.; Deval, J. The Ambiguous Base-Pairing and High Substrate Efficiency of T-705 (Favipiravir) Ribofuranosyl 5′-Triphosphate Towards Influenza A Virus Polymerase. *PLoS One* **2013**, *8*, e68347.
62. Abdelnabi, R.; de Morais, A. T. S.; Leyssen, P.; et al. Understanding the Mechanism of the Broad-Spectrum Antiviral Activity of Favipiravir (T-705): Key Role of the F1 Motif of the Viral Polymerase. *J. Virol.* **2017**, *91*, e00487–17.
63. Shannon, A.; Selisko, B.; Le, N. T. T.; et al. Rapid Incorporation of Favipiravir by the Fast and Permissive Viral RNA Polymerase Complex Results in SARS-CoV-2 Lethal Mutagenesis. *Nat. Commun.* **2020**, *11*, 4682.
64. Te Velthuis, A. J.; Arnold, J. J.; Cameron, C. E.; Van Den Worm, S. H.; Snijder, E. J. J. N. A. R. The RNA Polymerase Activity of SARS-Coronavirus nsp12 Is Primer Dependent. *Nucleic Acids Res.* **2010**, *38*, 203–214.
65. Cheng, A.; Zhang, W.; Xie, Y.; Jiang, W.; Arnold, E.; Sarafianos, S. G.; Ding, J. J. V. Expression, Purification, and Characterization of SARS Coronavirus RNA Polymerase. *Virology* **2005**, *335*, 165–176.
66. Huchting, J.; Winkler, M.; Nasser, H.; Meier, C. Synthesis of T-705-Ribonucleoside and T-705-Ribonucleotide and Studies of Chemical Stability. *ChemMedChem* **2017**, *12*, 652–659.
67. Dulin, D.; Arnold, J. J.; van Laar, T.; Oh, H. S.; Lee, C.; Perkins, A. L.; Harki, D. A.; Depken, M.; Cameron, C. E.; Dekker, N. H. Signatures of Nucleotide Analog Incorporation by an RNA-Dependent RNA Polymerase Revealed Using High-Throughput Magnetic Tweezers. *Cell Rep.* **2017**, *21*, 1063–1076.
68. Eckerle, L. D.; Lu, X.; Sperry, S. M.; et al. High Fidelity of Murine Hepatitis Virus Replication Is Decreased in nsp14 Exoribonuclease Mutants. *J. Virol.* **2007**, *81*, 12135–12144.
69. Smith, E. C.; Blanc, H.; Vignuzzi, M.; et al. Coronaviruses Lacking Exoribonuclease Activity Are Susceptible to Lethal Mutagenesis: Evidence for Proofreading And Potential Therapeutics. *PLOS Pathog.* **2013**, *9*, e1003565.
70. Sowa, T.; Ouchi, S. Facile Synthesis of 5′-Nucleotides by Selective Phosphorylation of a Primary Hydroxyl Group of Nucleosides with Phosphoryl Chloride. *Bull. Chem. Soc. Jpn.* **1975**, *48*, 2084–2090.
71. Cremosnik, G. S.; Hofer, A.; Jessen, H. J. J. A. C. I. E. Iterative Synthesis of Nucleoside Oligophosphates with Phosphoramidites. *Angew. Chem., Int. Ed.* **2014**, *53*, 286–289.
72. Meier, C. 2-Nucleos-5'-O-yl-4H-1,3,2-Benzodioxaphosphinin-2-Oxides—A New Concept for Lipophilic, Potential Prodrugs of Biologically Active Nucleoside Monophosphates. *Angew. Chem., Int. Ed.* **1996**, *35*, 70–72.
73. Meier, C.; De Clercq, E.; Balzarini, J. Nucleotide Delivery from *cyclo*Saligenyl-3'-Azido-3'-Deoxythymidine Monophosphates (*cyclo*Sal-AZTMP). *Eur. J. Org. Chem.* **1998**, 837–846.
74. Meier, C.; Ludek, O.; Krämer, T.; et al. Divergent Synthesis and Biological Evaluation of Carbocyclic α-, Iso- and 3′-Epi-Nucleosides and Their Lipophilic Nucleotide Prodrugs. *Synthesis* **2006**, *8*, 1313–1324.
75. Meier, C.; Lorey, M.; De Clercq, E.; Balzarini, J. *Cyclo*Sal-2',3'-Dideoxy-2', 3'-Didehydrothymidine Monophosphate (*cyclo*Sal-d4TMP): Synthesis and Antiviral Evaluation of a New d4TMP Delivery System. *J. Med. Chem.* **1998**, *41*, 1417–1427.
76. McGuigan, C.; Cahard, D.; Sheeka, H. M.; DeClercq, E.; Balzarini, J. Aryl Phosphoramidate Derivatives of d4T Have Improved Anti-HIV Efficacy in Tissue Culture and May Act by the Generation of a Novel Intracellular Metabolite. *J. Med. Chem.* **1996**, *39*, 1748–1753.

77. Balzarini, J.; Karlsson, A.; Aquaro, S.; Perno, C. F.; Cahard, D.; Naesens, L.; DeClercq, E.; McGuigan, C. Mechanism of Anti-HIV Action of Masked Alaninyl d4TMP Derivatives. *Proc. Natl. Acad. Sci. U. S. A.* **1996**, *93*, 7295–7299.
78. Balzarini, J.; Egberink, H.; Hartmann, K.; Cahard, D.; Vahlenkamp, T.; Thormar, H.; DeClercq, E.; McGuigan, C. Antiretrovirus Specificity and Intracellular Metabolism of 2′,3′-Didehydro-2′,3′-Dideoxythymidine (Stavudine) and Its 5′-Monophosphate Triester Prodrug So324. *Mol. Pharmacol.* **1996**, *50*, 1207–1213.
79. Girardet, J. L.; Perigaud, C.; Aubertin, A. M.; Gosselin, G.; Kirn, A.; Imbach, J. L. Increase of the Anti-HIV Activity of d4T in human T-Cell Culture by the Use of the Sate Pronucleotide Approach. *Bioorg. Med. Chem. Lett.* **1995**, *5*, 2981–2984.
80. Farquhar, D.; Khan, S.; Srivastva, D. N.; Saunders, P. P. Synthesis and Antitumor Evaluation of Bis[(Pivaloyloxy)Methyl] 2′-Deoxy-5-Fluorouridine 5′-Monophosphate (FdUMP)—A Strategy to Introduce Nucleotides into Cells. *J. Med. Chem.* **1994**, *37*, 3902–3909.
81. Farquhar, D.; Chen, R.; Khan, S. 5′-[4-(Pivaloyloxy)-1,3,2-Dioxaphosphorinan-2-Yl]-2′-Deoxy-5-Fluorouridine—A Membrane-Permeating Prodrug of 5-Fluoro-2′-Deoxyuridylic Acid (FdUMP). *J. Med. Chem.* **1995**, *38*, 488–495.
82. Briggs, A. D.; Camplo, M.; Freeman, S.; Lundstrom, J.; Pring, B. G. Acyloxymethyl and 4-Acyloxybenzyl Diester Prodrugs of Phosphonoformate. *Tetrahedron* **1996**, *52*, 14937–14950.
83. Lefebvre, I.; Perigaud, C.; Pompon, A.; Aubertin, A. M.; Girardet, J. L.; Kirn, A.; Gosselin, G.; Imbach, J. L. Mononucleoside Phosphotriester Derivatives with S-Acyl-2-Thioethyl Bioreversible Phosphate-Protecting Groups—Intracellular Delivery of 3′-Azido-2′,3′-Dideoxythymidine 5′-Monophosphate. *J. Med. Chem.* **1995**, *38*, 3941–3950.
84. Puech, F.; Gosselin, G.; Lefebvre, I.; Pompon, A.; Aubertin, A. M.; Kirn, A.; Imbach, J. L. Intracellular Delivery of Nucleoside Monophosphates through a Reductase-Mediated Activation Process. *Antivir. Res.* **1993**, *22*, 155–174.
85. Wagner, C. R.; Chang, S. L.; Griesgraber, G. W.; Song, H.; McIntee, E. J.; Zimmerman, C. L. Antiviral Nucleoside Drug Delivery via Amino Acid Phosphoramidates. *Nucleosides Nucleotides Nucleic Acids* **1999**, *18*, 913–919.
86. Meier, C.; Lomp, A.; Meerbach, A.; Wutzler, P. *Cyclo*Sal-BVDUMP Pronucleotides: How to Convert an Antiviral-Inactive Nucleoside Analogue into a Bioactive Compound against EBV. *J. Med. Chem.* **2002**, *45*, 5157–5172.
87. Meier, C. *Cyclo*Sal Phosphates as Chemical Trojan Horses for Intracellular Nucleotide and Glycosylmonophosphate Delivery—Chemistry Meets Biology. *Eur. J. Org. Chem.* **2006**, *5*, 1081–1102.
88. Meier, C. *Cyclo*Sal-Pronucleotides—Design of Chemical Trojan Horses. *Mini-Rev. Med. Chem.* **2002**, *2*, 219–234.
89. Meier, C.; Habel, L.; Haller-Meier, F.; Lomp, A.; Herderich, M.; Klocking, R.; Meerbach, A.; Wutzler, P. Chemistry and Anti-Herpes Simplex Virus Type 1 Evaluation of *cyclo*Sal-Nucleotides of Acyclic Nucleoside Analogues. *Antivir. Chem. Chemother.* **1998**, *9*, 389–402.
90. Meier, C.; Balzarini, J. Application of the *cyclo*Sal-Prodrug Approach for Improving the Biological Potential of Phosphorylated Biomolecules. *Antivir. Res.* **2006**, *71*, 282–292.
91. Meier, C.; Ruppel, M. F. H.; Vukadinovic, D.; Balzarini, J. Second Generation of *cyclo*Sal-Pronucleotides with Esterase-Cleavable Sites: The "Lock-in"-Concept. *Nucleosides Nucleotides Nucleic Acids* **2004**, *23*, 89–115.
92. Gisch, N.; Balzarini, J.; Meier, C. Enzymatically Activated *cyclo*Sal-d4T-Monophosphates: The Third Generation of *cyclo*Sal-Pronucleotides. *J. Med. Chem.* **2007**, *50*, 1658–1667.

93. Meier, C.; Knispel, T.; DeClercq, E.; Balzarini, J. ADA-Bypass by Lipophilic *cyclo*Sal-ddAMP pro-Nucleotides a Second Example of the Efficiency of the *cyclo*Sal-Concept. *Bioorg. Med. Chem. Lett.* **1997**, *7*, 1577–1582.
94. Meier, C.; Knispel, T.; De Clercq, E.; Balzarini, J. *Cyclo*Sal-Pronucleotides of 2′,3′-Dideoxyadenosine and 2′,3′-Dideoxy-2′,3′-Didehydroadenosine: Synthesis and Antiviral Evaluation of a Highly Efficient Nucleotide Delivery System. *J. Med. Chem.* **1999**, *42*, 1604–1614.
95. Lorey, M.; Meier, C.; DeClercq, E.; Balzarini, J. New Synthesis and Antitumor Activity of *cyclo*Sal-Derivatives of 5-Fluoro-2′-Deoxyuridinemonophosphate. *Nucleosides Nucleotides Nucleic Acids* **1997**, *16*, 789–792.
96. Lorey, M.; Meier, C.; DeClercq, E.; Balzarini, J. *Cyclo*-Saligenyl-5-Fluoro-2′-Deoxyuridinemonophosphate (*cyclo*Sal-FdUMP)—A New Prodrug Approach for FdUMP. *Nucleosides Nucleotides Nucleic Acids* **1997**, *16*, 1307–1310.
97. Meier, C.; DeClercq, E.; Balzarini, J. *Cyclo*-Saligenyl-3′-Azido-2′,3′-Dideoxy-Thymidinemonophosphate (*cyclo*Sal-AZTMP)—A New pro-Nucleotide Approach. *Nucleosides Nucleotides Nucleic Acids* **1997**, *16*, 793–796.
98. Balzarini, J.; Naesens, L.; Aquaro, S.; Knispel, T.; Perno, C. F.; De Clercq, E.; Meier, C. Intracellular Metabolism of *cyclo*Saligenyl 3'-Azido-2',3'-Dideoxythymidine Monophosphate, a Prodrug of 3'-Azido-2',3'-Dideoxythymidine (Zidovudine). *Mol. Pharmacol.* **1999**, *56*, 1354–1361.
99. Mazzon, C.; Rampazzo, C.; Scaini, M. C.; Gallinaro, L.; Karlsson, A.; Meier, C.; Balzarini, J.; Reichard, P.; Bianchi, V. Cytosolic and Mitochondrial Deoxyribonucleotidases: Activity with Substrate Analogs, Inhibitors and Implications for Therapy. *Biochem. Pharmacol.* **2003**, *66*, 471–479.
100. Furman, P. A.; Fyfe, J. A.; Stclair, M. H.; Weinhold, K.; Rideout, J. L.; Freeman, G. A.; Lehrman, S. N.; Bolognesi, D. P.; Broder, S.; Mitsuya, H.; Barry, D. W. Phosphorylation of 3′-Azido-3′-Deoxythymidine and Selective Interaction of the 5′-Triphosphate with Human-Immunodeficiency-Virus Reverse-Transcriptase. *Proc. Natl. Acad. Sci. U. S. A.* **1986**, *83*, 8333–8337.
101. Balzarini, J.; Herdewijn, P.; Declercq, E. Differential Patterns of Intracellular Metabolism of 2′,3′-Didehydro-2′,3′-Dideoxythymidine and 3′-Azido-2′,3′-Dideoxythymidine, 2 Potent Anti-Human Immunodeficiency Virus Compounds. *J. Biol. Chem.* **1989**, *264*, 6127–6133.
102. Hostetler, K. Y.; Stuhmiller, L. M.; Lenting, H. B. M.; Vandenbosch, H.; Richman, D. D. Synthesis and Antiretroviral Activity of Phospholipid Analogs of Azidothymidine and Other Antiviral Nucleosides. *J. Biol. Chem.* **1990**, *265*, 6112–6117.
103. Vanwijk, G. M. T.; Hostetler, K. Y.; Vandenbosch, H. Lipid Conjugates of Antiretroviral Agents—Release of Antiretroviral Nucleoside Monophosphates by a Nucleoside Diphosphate Diglyceride Hydrolase Activity from Rat-Liver Mitochondria. *Biochim. Biophys. Acta* **1991**, *1084*, 307–310.
104. Hostetler, K. Y.; Richman, D. D.; Carson, D. A.; Stuhmiller, L. M.; Vanwijk, G. M. T.; Vandenbosch, H. Greatly Enhanced Inhibition of Human-Immunodeficiency-Virus Type-1 Replication in Cem and Ht4-6c Cells by 3′-Deoxythymidine Diphosphate Dimyristoylglycerol, a Lipid Prodrug of 3′-Deoxythymidine. *Antimicrob. Agents Chemother.* **1992**, *36*, 2025–2029.
105. Hostetler, K. Y.; Parker, S.; Sridhar, C. N.; Martin, M. J.; Li, J. L.; Stuhmiller, L. M.; Vanwijk, G. M. T.; Vandenbosch, H.; Gardner, M. F.; Aldern, K. A.; Richman, D. D. Acyclovir Diphosphate Dimyristoylglycerol—A Phospholipid Prodrug with Activity against Acyclovir-Resistant Herpes-Simplex Virus. *Proc. Natl. Acad. Sci. U. S. A.* **1993**, *90*, 11835–11839.

106. Bonnaffe, D.; Dupraz, B.; Ughetto-Monfrin, J.; et al. Synthesis of Acyl Pyrophosphates - Application to the Synthesis of Nucleotide Lipophilic Prodrugs. *Tetrahedron Lett.* **1995**, *36*, 531–534.
107. Bonnaffe, D.; Dupraz, B.; Ughetto-Monfrin, J.; et al. Synthesis of Nucleotide Lipophilic Prodrugs Containing 2 Inhibitors Targeted against Different Phases of the HIV Replication Cycle. *Nucleosides, Nucleotides Nucleic Acids* **1995**, *14*, 783–787.
108. Bonnaffe, D.; Dupraz, B.; Ughetto-Monfrin, J.; et al. Potential Lipophilic Nucleotide Prodrugs: Synthesis, Hydrolysis, and Antiretroviral Activity of AZT and d4T Acyl Nucleotides. *J. Org. Chem.* **1996**, *61*, 895–902.
109. Thomson, W.; Nicholls, D.; Irwin, W. J.; et al. Synthesis, Bioactivation and Anti-HIV Activity of the Bis(4-Acyloxybenzyl) and Mono(4-Acyloxybenzyl) Esters of the 5′-Monophosphate of AZT. *J. Chem. Soc. Perkin Trans.* **1993**, *11*, 1239–1245.
110. Jessen, H. J.; Schulz, T.; Balzarini, J.; Meier, C. Bioreversible Protection of Nucleoside Diphosphates. *Angew. Chem., Int. Ed.* **2008**, *47*, 8719–8722.
111. Pertenbreiter, F.; Balzarini, J.; Meier, C. Nucleoside Mono- and Diphosphate Prodrugs of 2', 3'-Dideoxyuridine and 2', 3'-Dideoxy-2', 3'-Didehydrouridine. *ChemMedChem* **2015**, *10*, 94–106.
112. Schulz, T.; Balzarini, J.; Meier, C. The Di*PP*ro Approach: Synthesis, Hydrolysis, and Antiviral Activity of Lipophilic d4T Diphosphate Prodrugs. *ChemMedChem* **2014**, *9*, 762–775.
113. Weinschenk, L.; Schols, D.; Balzarini, J.; Meier, C. Nucleoside Diphosphate Prodrugs: Nonsymmetric Di*PP*ro-Nucleotides. *J. Med. Chem.* **2015**, *58*, 6114–6130.
114. Meier, C.; Jessen, H. J.; Schulz, T.; Weinschenk, L.; Pertenbreiter, F.; Balzarini, J. Rational Development of Nucleoside Diphosphate Prodrugs: Di*PP*ro-Compounds. *Curr. Med. Chem.* **2015**, *22*, 3933–3950.
115. Weinschenk, L.; Gollnest, T.; Schols, D.; Balzarini, J.; Meier, C. Bis(Benzoyloxybenzyl)-Di*PP*ro Nucleoside Diphosphates of Anti-HIV Active Nucleoside Analogues. *ChemMedChem* **2015**, *10*, 891–900.
116. Zhu, Y. L.; Dutschman, G. E.; Liu, S. H.; Bridges, E. G.; Cheng, Y. C. Anti-Hepatitis B Virus Activity and Metabolism of 2',3'-Dideoxy-2',3'-Didehydro-beta-L(−)-5-Fluorocytidine. *Antimicrob. Agents Chemother.* **1998**, *42*, 1805–1810.
117. Kreimeyer, A.; Andre, F.; Gouyette, C.; Huynh-Dinh, T. Transmembrane Transport of Adenosine 5'-Triphosphate Using a Lipophilic Cholesteryl Derivative. *Angew. Chem., Int. Ed.* **1998**, *37*, 2853–2855.
118. Bonnaffe, D.; Dupraz, B.; Ughettomonfrin, J.; Namane, A.; Dinh, T. H. Synthesis of Acyl Pyrophosphates—Application to the Synthesis of Nucleotide Lipophilic Prodrugs. *Tetrahedron Lett.* **1995**, *36*, 531–534.
119. Vanwijk, G. M. T.; Hostetler, K. Y.; Kroneman, E.; Richman, D. D.; Sridhar, C. N.; Kumar, R.; Vandenbosch, H. Synthesis and Antiviral Activity of 3′-Azido-3′-Deoxythymidine Triphosphate Distearoylglycerol—A Novel Phospholipid Conjugate of the Anti-HIV Agent AZT. *Chem. Phys. Lipids* **1994**, *70*, 213–222.
120. Bonnaffe, D.; Dupraz, B.; Ughettomonfrin, J.; Namane, A.; Dinh, T. H. Synthesis of Nucleotide Lipophilic Prodrugs Containing 2 Inhibitors Targeted against Different Phases of the HIV Replication Cycle. *Nucleosides Nucleotides Nucleic Acids* **1995**, *14*, 783–787.
121. Bonnaffe, D.; Dupraz, B.; UghettoMonfrin, J.; Namane, A.; Henin, Y.; Dinh, T. H. Potential Lipophilic Nucleotide Prodrugs: Synthesis, Hydrolysis, and Antiretroviral Activity of AZT and d4T Acyl Nucleotides. *J. Organomet. Chem.* **1996**, *61*, 895–902.
122. Gollnest, T.; de Oliveira, T. D.; Schols, D.; Balzarini, J.; Meier, C. Lipophilic Prodrugs of Nucleoside Triphosphates as Biochemical Probes and Potential Antivirals. *Nat. Commun.* **2015**, *6*, 8716.

123. Gollnest, T.; de Oliveira, T. D.; Rath, A.; Hauber, I.; Schols, D.; Balzarini, J.; Meier, C. Membrane-Permeable Triphosphate Prodrugs of Nucleoside Analogues. *Angew. Chem. Int. Ed.* **2016**, *55*, 5255–5258.
124. Mohamady, S.; Jakeman, D. L. An Improved Method for the Synthesis of Nucleoside Triphosphate Analogues. *J. Organomet. Chem.* **2005**, *70*, 10588–10591.
125. Mohamady, S.; Taylor, S. D. General Procedure for the Synthesis of Dinucleoside Polyphosphates. *J. Organomet. Chem.* **2011**, *76*, 6344–6349.
126. Jia, X.; Schols, D.; Meier, C. Anti-HIV-Active Nucleoside Triphosphate Prodrugs. *J. Med. Chem.* **2020**, *63*, 6003–6027.
127. Jia, X.; Schols, D.; Meier, C. Lipophilic Triphosphate Prodrugs of Various Nucleoside Analogues. *J. Med. Chem.* **2020**, *63*, 6991–7007.
128. Zhao, C. L.; Jia, X.; Schols, D.; Balzarini, J.; Meier, C. γ-Non-Symmetrically Dimasked Tri*PPP*ro-Prodrugs as Potential Antiviral Agents against HIV. *ChemMedChem* **2020**, *16*, 499–512.